International Journal of Bifurcation and Chaos, Vol. 14, No. 5 (2004) 1507–1537

A NEW CHAOTIC SYSTEM AND BEYOND: THE GENERALIZED LORENZ-LIKE SYSTEM

JINHU LÜ
Institute of Systems Science,
Academy of Mathematics and Systems Science,
Chinese Academy of Sciences, Beijing 100080, P. R. China
jhlu@mail.iss.ac.cn

GUANRONG CHEN
Department of Electronic Engineering,
City University of Hong Kong, Kowloon, Hong Kong, P. R. China
gchen@ee.cityu.edu.hk

DAIZHAN CHENG
Institute of Systems Science,
Academy of Mathematics and Systems Science,
Chinese Academy of Sciences, Beijing 100080, P. R. China
dcheng@iss03.iss.ac.cn

Received January 6, 2003; Revised February 13, 2003

This article introduces a new chaotic system of three-dimensional quadratic autonomous ordinary differential equations, which can display (i) two 1-scroll chaotic attractors simultaneously, with only three equilibria, and (ii) two 2-scroll chaotic attractors simultaneously, with five equilibria. Several issues such as some basic dynamical behaviors, routes to chaos, bifurcations, periodic windows, and the compound structure of the new chaotic system are then investigated, either analytically or numerically. Of particular interest is the fact that this chaotic system can generate a complex 4-scroll chaotic attractor or confine two attractors to a 2-scroll chaotic attractor under the control of a simple constant input. Furthermore, the concept of generalized Lorenz system is extended to a new class of generalized Lorenz-like systems in a canonical form. Finally, the important problems of classification and normal form of three-dimensional quadratic autonomous chaotic systems are formulated and discussed.

Keywords: Multi-scroll chaotic attractor; chaotification; three-dimensional quadratic autonomous system; Lorenz-like system; normal form.

1. Introduction

Chaos as a very interesting complex nonlinear phenomenon has been intensively studied in the last four decades within the science, mathematics and engineering communities.

Recently, chaos has been found to be very useful and has great potential in many technological disciplines such as in information and computer sciences, power systems protection, biomedical systems analysis, flow dynamics and liquid mixing, encryption and communications, and so on [Chen & Dong, 1998; Chen, 1999; Lü *et al.*, 2002e; Chen & Lü, 2003, and references therein]. Therefore, academic research on chaotic dynamics has evolved from the traditional trend of analyzing and

understanding chaos [Hao, 1984] to the new direction of controlling and utilizing it [Ott *et al.*, 1990; Chen, 1993; Chen & Dong, 1998; Chen, 1999; Wang & Chen, 2000; Lü *et al.*, 2002e; Chen & Lü, 2003]. In a broader sense, chaos control can be divided into two categories: one is to suppress the chaotic dynamical behavior when it is harmful [Ott *et al.*, 1990; Chen, 1993], and the other is to create or enhance chaos when it is desirable — known as chaotification or anticontrol of chaos [Chen & Lai, 1998; Chen & Dong, 1998; Wang & Chen, 1999; Wang *et al.*, 2000; Lü *et al.*, 2002f; Chen & Lü, 2003; Lü *et al.*, 2003]. Very recently, there has been increasing interest in exploiting chaotic dynamics in engineering applications, where some attention has been focused on effectively creating chaos via simple physical systems such as electronic circuits [Tang *et al.*, 2001; Wang & Chen, 2000] and switching piecewise-linear controllers [Lü *et al.*, 2002f; Lü *et al.*, 2003].

Chaotification is a very attractive theoretical subject, which however is quite challenging technically. This is because it involves creating some very complicated but well-organized dynamical behaviors, which usually also involves bifurcations or fractals. For a given system, which may be linear or nonlinear and originally may even be stable, the question is how to generate chaos out of it, by using a simple and easily implementable controller such as a state or output feedback controller, or using an accessible parameter tuner. During the last few years, a great deal of effort has been made toward this goal, not only via computer simulations but also by development of rigorous mathematical theories. In the endeavor of chaotification, purposefully creating discrete chaos has gained great success [Chen & Lai, 1998; Wang & Chen, 1999]. At the same time, chaotification in continuous-time systems is also developing rapidly. For example, a simple linear partial state-feedback controller is able to drive the Lorenz system [Lorenz, 1963] from its nonchaotic state to chaotic state. This engineering design has led to the discovery of the chaotic Chen system [Chen & Ueta, 1999], which is a *dual* of the Lorenz system [Čelikovský & Chen, 2002, 2003], and led to the discovery of a transition system between the Lorenz system and the Chen system [Lü & Chen, 2002].

In 1963, Lorenz discovered chaos in a simple system of three autonomous ordinary differential equations that has only two quadratic nonlinearities, in order to describe the simplified Rayleigh–Bénard problem [Festa *et al.*, 2002]. It is notable that the Lorenz system has seven terms on the right-hand side, two of which are nonlinear (xz and xy). In 1976, Rössler found a three-dimensional quadratic autonomous chaotic system [Rössler, 1976], which also has seven terms on the right-hand side, but with only one quadratic nonlinearity (xz). Obviously, the Rössler system has a simpler algebraic structure as compared to the Lorenz system.

It was believed that the Rössler system might be the simplest possible chaotic flow [Lorenz, 1993], where the simplicity refers to the algebraic representation rather than the physical process described by the equations or the topological structure of the strange attractor. It is therefore interesting to ask whether or not there are three-dimensional autonomous chaotic systems with fewer than seven terms including only one or two quadratic nonlinearities? The fact is that Rössler actually had produced another even simpler chaotic system in 1979, which has only six terms with a single quadratic nonlinearity (y^2) [Rössler, 1979]. Thus, the question becomes "How complicated must a three-dimensional autonomous system be in order to produce chaos?" The well-known Poincaré–Bendixson theorem shows that chaos does not exist in a two-dimensional continuous-time autonomous system (or a second-order equation) [Wiggins, 1990]. Therefore, a necessary condition for a continuous-time autonomous system to be chaotic is to have three variables with at least one nonlinear term. As a side note, it is also known that there is a direct connection between three-dimensional quadratic chaotic systems and Lagrangian mixing [Schmalzl *et al.*, 1995; Funakoshi, 2001]. Lagrangian mixing poses some interesting questions about dynamical systems; however, since realistic models are mainly experimental and numerical, this subject is still in its early involving phase of development.

Three-dimensional quadratic autonomous systems are very important for studying bifurcations, limit cycles and chaotic flows. Recently, it is proved [Zhang & Jack, 1997] that three-dimensional dissipative quadratic systems of ordinary differential equations, with a total of four terms on the right-hand side, cannot exhibit chaos. Very recently, this result was extended to three-dimensional conservative quadratic systems [Jack & Zhang, 1999; Yang & Chen, 2002]. Later, it was known that autonomous chaotic flow could be produced by

a three-dimensional quadratic autonomous system having five terms on the right-hand side, with at least one quadratic nonlinearity, or having six terms with a single quadratic nonlinearity. Lately, chaotic flow in an algebraically simplest three-dimensional quadratic autonomous system was found by using jerky functions [Sprott & Linz, 2000], which has only five terms with a single quadratic nonlinearity (y^2). In fact, this system is simpler than any others previously found, regarding both its jerky representation and its representation as a dynamical system.

However, it is noticed that the simplicity of a system can be measured in various ways. Algebraic simplicity of system's structure is one way, and topological simplicity of chaotic attractor is another. Rössler's attractor and most of Sprott's examples are topologically simpler than the two-scroll Lorenz attractor [Sprott, 1994, 1997; Sprott & Linz, 2000]. In fact, Rössler attractor has a single-fold band structure. Furthermore, its one-scroll structure is the simplest topological structure for a three-dimensional quadratic autonomous chaotic system. Thus, it is interesting to ask whether or not there are three-dimensional quadratic autonomous chaotic systems that can display attractors with more complex topological structures than the two-scroll Lorenz attractor. That is, "Is the two-scroll Lorenz attractor the most complex topological structure of this class of chaotic systems?" The answer is *no*. In fact, the recently discovered Chen attractor and its associate transition attractor have more complex topological structures than the original Lorenz attractor [Ueta & Chen, 2000; Lü & Chen, 2002]. Nevertheless, these newly found attractors also have two-scrolls but not more than that.

Therefore, in combining these two points of views on simplicity (or complexity) of a chaotic system, it would be truly interesting to seek for lower-dimensional chaotic systems that have a simple algebraic system structure but with a complex topological attractor structure. This is not just for theoretical interest; such chaotic systems would be useful in some engineering applications such as secure communications.

In the endeavor of finding three-dimensional quadratic autonomous chaotic systems, other than luckily encountering chaos in unexpected simulations or experiments, there seems to be two sensible methods: one is Sprott's exhaustive searching via computer programming [Sprott, 1994], and the other is Chen's theoretical approach via chaotification [Chen & Lai, 1998; Wang & Chen, 1999; Chen & Ueta, 1999; Lü & Chen, 2002].

For nearly 40 years, one of the classic icons of modern nonlinear dynamics has been the Lorenz attractor. In 2000, Smale described eighteen challenging mathematical problems for the twenty-first century [Smale, 2000], in which the fourteenth problem is about the Lorenz attractor. In this regard, one concerned problem has been: "Does it really exist?" Only very recently, the Lorenz attractor was mathematically confirmed to exist [Tucker, 1999; Steward, 2000]. Another interesting question regarding chaotic systems is: "How complex can the topological structure of the chaotic attractor, if exists, of a three-dimensional quadratic autonomous system be?" Here, it is noted that the complexity of the topological structure of a chaotic attractor may be measured in two aspects: the number of subattractors and the number of parts ("scrolls" or "wings") of the attractor.

It has been well known that piecewise-linear functions can generate n-scroll attractors in Chua's circuit [Suykens & Vandewalle, 1993; Elwakil *et al.*, 2001; Elwakil *et al.*, 2002], and in a circuit with the absolute value as the only nonlinearity, they can also create a complex n-scroll chaotic attractor [Tang *et al.*, 2002]. Recently, Liu and Chen [2003] found a simple three-dimensional quadratic autonomous chaotic system, which can display a 2-scroll and also (visually) a 4-scroll attractor. Motivated by these works, this article introduces one more simple three-dimensional quadratic autonomous system, which can generate two 1-scroll chaotic attractors simultaneously, or two complex 2-scroll chaotic attractors simultaneously. It is believed that a three-dimensional quadratic autonomous chaotic system can have at most two chaotic attractors simultaneously, and the system to be discussed here is one such simple but interesting chaotic system.

More precisely, the objective of this article is to present and further study a simple, interesting, and yet complex three-dimensional quadratic autonomous chaotic system, which can display two 1-scroll attractors simultaneously or two complex 2-scroll chaotic attractors simultaneously. This new chaotic system is introduced in Sec. 2. Section 3 explains how to find this new chaotic system, and Sec. 4 further investigates the dynamical behaviors of this chaotic system, by employing some tools used

in [Ueta & Chen, 2000; Lü *et al.*, 2002b]. The compound structure of chaotic attractors [Elwakil & Kennedy, 2001; Lü *et al.*, 2002c, 2002g] is analyzed for the two 2-scroll attractor of this new system in Sec. 5. Then, Secs. 6 and 7 explore the relationship and connecting function for the 2-scroll attractor. The concept of generalized Lorenz system [Čelikovský & Chen, 2002, 2003] is then extended, and a class of generalized Lorenz-like systems are defined and discussed in Sec. 8. Furthermore, classification and normal form of three-dimensional quadratic autonomous chaotic systems are studied in Sec. 9. Finally, conclusions and discussions are given in Sec. 10, with a rather detailed list of references provided at the end of the article.

2. A New Chaotic System

Consider the following simple three-dimensional quadratic autonomous system, which can display two chaotic attractors simultaneously:

$$\begin{cases} \dot{x} = -\dfrac{ab}{a+b}x - yz + c \\ \dot{y} = ay + xz \\ \dot{z} = bz + xy\,, \end{cases} \tag{1}$$

where a, b, c are real constants.

This system is found to be chaotic in a wide parameter range and has many interesting complex dynamical behaviors. For example, it is chaotic for the parameters $a = -10$, $b = -4$, and $|c| < 19.2$, and for $a = -10$, $b = -4$, $c = 18.1$, it displays two 1-scroll chaotic attractors as shown in Fig. 1.

The Lyapunov exponent spectrum of system (1) is found to be $\lambda_1 = 0.253223$, $\lambda_2 = 0$, $\lambda_3 = -11.3944$, and the Lyapunov dimension is $d_L = 2.0221$ for initial value (1, 1, 1). Obviously, when $a = -10$, $b = -4$, $c = 18.1$, the system has only three equilibria:

$$E_1(-6.335,\, 0,\, 0)\,,$$

$$E_2\left(2\sqrt{10},\ \sqrt{\frac{80}{7} + 3.62\sqrt{10}},\ \frac{1}{2}\sqrt{\frac{800}{7} + 36.2\sqrt{10}}\right),$$

$$E_3\left(2\sqrt{10},\ -\sqrt{\frac{80}{7} + 3.62\sqrt{10}},\ -\frac{1}{2}\sqrt{\frac{800}{7} + 36.2\sqrt{10}}\right).$$

It is a strange phenomenon to have two coexisting chaotic attractors in a three-dimensional quadratic autonomous chaotic system with only three equilibria.

Furthermore, when $a = -10$, $b = -4$, $c = 0$, this system can display two complex 2-scroll chaotic attractors, as shown in Fig. 2. According to their geometric locations, these two coexisting attractors are called upper-attractor and lower-attractor here for convenience.

For three-dimensional autonomous systems, Vaněček and Čelikovský [1996] gave a classification in terms of $a_{12}a_{21}$, where a_{12}, a_{21} are the corresponding entries of the linear part of the system described by the constant matrix $A = [a_{ij}]_{3\times3}$. According to this condition, the Lorenz system satisfies

$$a_{12}a_{21} > 0\,,$$

the Chen system satisfies

$$a_{12}a_{21} < 0\,,$$

and system (1) here satisfies

$$a_{12}a_{21} = 0\,.$$

This is similar to the system studied in [Lü & Chen, 2002] and then further discussed in [Čelikovský & Chen, 2002]. This means that system (1) is also a transition system that bridges the gap between the Lorenz and Chen systems. However, system (1) has similar but different dynamical behaviors with the transition system found by Lü and Chen [2002], investigated in [Lü *et al.*, 2002b].

By a suitable nonsingular transform, it is assumed without loss of generality that $A = [a_{ij}]_{3\times3} = \mathrm{diag}\{a, b, c\}$. In this setting, Liu and Chen [2003] derived another classification condition in terms of $ab + ac + bc$ for the three-dimensional quadratic autonomous systems. Using this condition, the 4-scroll system discovered in [Liu & Chen, 2003] satisfies

$$ab + ac + bc \neq 0\,,$$

while system (1) here satisfies

$$ab + ac + bc = 0\,.$$

Therefore, system (1) is a new and particular system that satisfies two different classification conditions as described above. Moreover, this system has many interesting complex dynamical behaviors, as will be seen below.

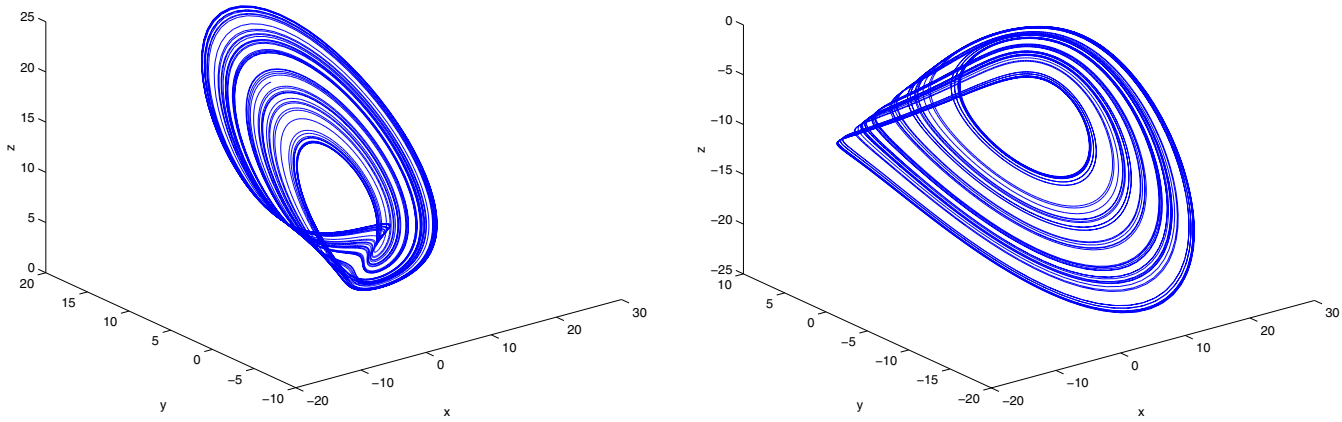

(a) (b)

Fig. 1. Two coexisting 1-scroll chaotic attractors. (a) Initial value $(x_0, y_0, z_0)(z_0 > 0)$, (b) initial value $(x_0, y_0, z_0)(z_0 < 0)$. $(a = -10, b = -4, c = 18.1.)$

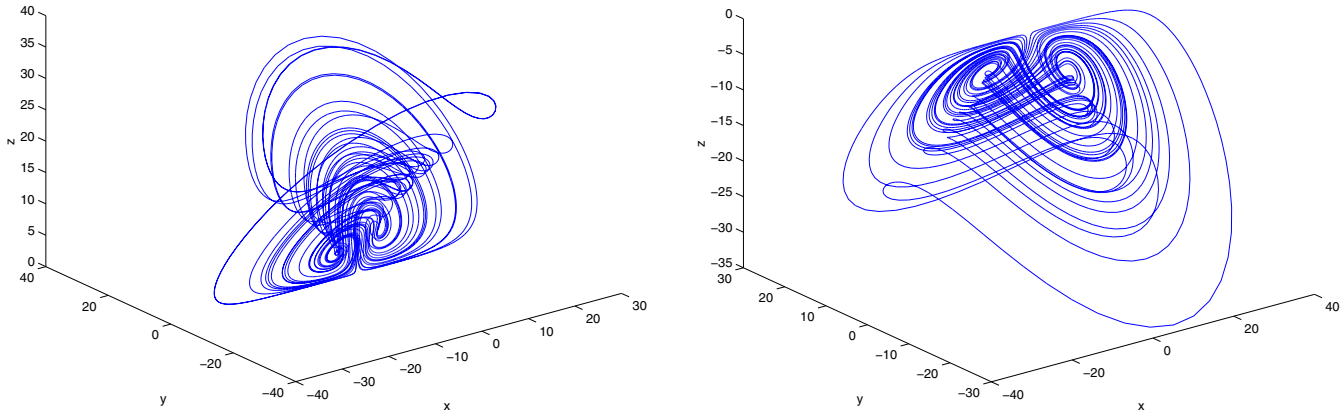

(a) (b)

Fig. 2. Two coexisting 2-scroll chaotic attractors. (a) Upper-attractor, (b) lower-attractor. $(a = -10, b = -4, c = 0.)$

3. The Upper-Attractor and Lower-Attractor

This section provides a brief discussion of how the idea of chaotification leads to the discovery of the system (1) that has two coexisting 2-scroll chaotic attractors.

Start with the following general form of a three-dimensional quadratic autonomous system:

$$\begin{cases} \dot{x} = -\dfrac{ab}{a+b}x + c + dyz \\ \dot{y} = ay + exz \\ \dot{z} = bz + fxy\,, \end{cases} \tag{2}$$

where a, b, c, d, e, f are all real constant parameters.

The system Jacobian, evaluated at (x_0, y_0, z_0), is given by

$$J_{(x_0,y_0,z_0)} = \begin{pmatrix} -\dfrac{ab}{a+b} & dz_0 & dy_0 \\ ez_0 & a & ex_0 \\ fy_0 & fx_0 & b \end{pmatrix}. \tag{3}$$

To find the equilibria of system (2), let

$$\frac{dx}{dt} = \frac{dy}{dt} = \frac{dz}{dt} = 0\,. \tag{4}$$

Clearly, if

$$\frac{ab}{ef} > 0, \quad A = -\frac{ab^2}{(a+b)df} + \frac{bc}{df}\sqrt{\frac{ef}{ab}} > 0\,,$$

and

$$B = -\frac{ab^2}{(a+b)df} - \frac{bc}{df}\sqrt{\frac{ef}{ab}} \le 0\,,$$

then there exist three equilibria:

$$S_1\left(\frac{(a+b)c}{ab},\, 0,\, 0\right)$$
$$S_2\left(x_+,\, \sqrt{A},\, -\frac{f}{b}\sqrt{A}x_+\right)$$
$$S_3\left(x_+,\, -\sqrt{A},\, \frac{f}{b}\sqrt{A}x_+\right);$$

if $ab/ef > 0$, $A \le 0$, and $B > 0$, then system (2) has another set of three equilibria:

$$S_1\left(\frac{(a+b)c}{ab},\, 0,\, 0\right)$$
$$S_4\left(x_-,\, \sqrt{B},\, -\frac{f}{b}\sqrt{B}\,x_-\right)$$
$$S_5\left(x_-,\, -\sqrt{B},\, \frac{f}{b}\sqrt{B}\,x_-\right);$$

yet if $ab/ef > 0$, $A > 0$, and $B > 0$, then system (2) has five equilibria: S_1, S_2, S_3, S_4, S_5; but if $ab/ef > 0$, $A < 0$, and $B < 0$, or $ab/ef \le 0$, then the system has a unique equilibrium S_1, where $x_\pm = \pm\sqrt{ab/ef}$.

In order to ensure system (2) be chaotic, just like the typical three-dimensional autonomous chaotic systems such as the Lorenz system, it is required that

- system (2) is dissipative, that is, $\Delta V = (\partial\dot{x}/\partial x) + (\partial\dot{y}/\partial y) + (\partial\dot{z}/\partial z) = -(ab/(a+b)) + a + b = (a^2 + ab + b^2)/(a+b) < 0$;
- system (2) has three or five equilibria, and all these equilibria are unstable.

It is noticed that a three-dimensional conservative quadratic autonomous system can also display chaos. Indeed, Sprott [1997] found an example of three-dimensional conservative autonomous chaotic system. Here, only the dissipative system case is discussed.

Since $a^2 + ab + b^2 = (a + (1/2)b)^2 + (3b^2/4) > 0$, one has $a + b < 0$. When $ab/ef > 0$ and A, B are not simultaneously zero, system (2) has three or five equilibria. We may choose $|d| = 1$, $|e| = 1$, $|f| = 1$ for the simplicity because the constants d, e, f determine the sign of the quadratic items. To have chaotic behavior, these equilibria cannot be stable, that is, the Jacobian should have at least one unstable eigenvalue when it is evaluated at each of these equilibria. Thus, theoretical analysis and various trial tests reveal two sets of parameters:

- $a < 0$, $b < 0$, $c \in \mathbf{R}$, $d = -1$, $e = 1$, $f = 1$
- $a < 0$, $b < 0$, $c \in \mathbf{R}$, $d = 1$, $e = -1$, $f = -1$,

which yield the new chaotic system (1) and the following system:

$$\begin{cases} \dot{x} = -\dfrac{ab}{a+b}x + c + yz \\ \dot{y} = ay - xz \\ \dot{z} = bz - xy\,. \end{cases} \tag{5}$$

It is noticed that systems (1) and (5) are equivalent under the transformation $(x, y, z) \to (-x, y, z)$. In the following, therefore, only system (1) is considered.

Furthermore, for simplicity, assume $c = 0$, which yields the following system:

$$\begin{cases} \dot{x} = -\dfrac{ab}{a+b}x - yz \\ \dot{y} = ay + xz \\ \dot{z} = bz + xy\,, \end{cases} \tag{6}$$

where a, b are real constants. This is the system to be further analyzed in the rest of this article.

First, Fig. 2 shows the two coexisting 2-scroll chaotic attractors — upper-attractor and lower-attractor — of system (6). More detailed dynamical behaviors of system (6) will be further investigated in the following sections.

4. Dynamical Behaviors of the New Chaotic System

4.1. *Some basic properties*

System (6) shares various properties with some known three-dimensional quadratic autonomous systems, such as the Lorenz system. These are listed in the following:

4.1.1. *Symmetry and invariance*

First, note the invariance of the system under the transforms $(x, y, z) \to (x, -y, -z)$, $(x, y, z) \to (-x, -y, z)$, and $(x, y, z) \to (-x, y, -z)$. That is, system (6) is symmetrical about the three coordinate axes x, y, z, respectively. Furthermore, these symmetries persist for all values of the system parameters. Also, it is clear that the three coordinate axes x, y, z themselves are solution orbits of

the system. Moreover, the orbits on the y-axis and z-axis tend to the origin, while the orbits on the x-axis tend to infinity, as $t \to \infty$. This chaotic system is robust to various small perturbations due to its highly symmetric structure.

4.1.2. *Dissipativity and existence of attractor*

For system (6), it is noticed that

$$\nabla V = \frac{\partial \dot{x}}{\partial x} + \frac{\partial \dot{y}}{\partial y} + \frac{\partial \dot{z}}{\partial z} = -\frac{ab}{a+b} + a + b$$

$$= \frac{\left(a + \frac{1}{2}b\right)^2 + \frac{3}{4}b^2}{a+b}\,.$$

So, when $a + b < 0$, system (6) is dissipative, with an exponential contraction rate:

$$\frac{dV}{dt} = \frac{a^2 + ab + b^2}{a+b}\,V\,.$$

That is, a volume element V_0 is contracted by the flow into a volume element $V_0 e^{\frac{a^2+ab+b^2}{a+b}t}$ in time t. This means that each volume containing the system trajectory shrinks to zero as $t \to \infty$ at an exponential rate, $(a^2 + ab + b^2)/(a + b)$. Therefore, all system orbits are ultimately confined to a specific subset of zero volume, and the asymptotic motion settles onto an attractor.

4.1.3. *Diffeomorphism and topological equivalence*

Theorem 1. *System (1) is not diffeomorphic and, further, not topologically equivalent with any known three-dimensional quadratic autonomous chaotic system.*

Proof. For simplicity of notation and discussion, denote any of the known three-dimensional quadratic autonomous chaotic system, e.g. the Lorenz system, by

$$\dot{x} = f(x)\,, \tag{7}$$

and the new chaotic system (1), by

$$\dot{y} = g(y)\,. \tag{8}$$

If the numbers of equilibria for systems (7) and (8) are not the same, then they are not diffeomorphic. For example, the Lorenz system has three equilibria, while system (1) with two 2-scroll attractors has five equilibria. So they are not diffeomorphic.

If the numbers of subattractors for systems (7) and (8) are not the same, then they are not diffeomorphic. For example, the Lorenz system has a single 2-scroll chaotic attractor, while system (1) with three equilibria has two coexisting 1-scroll chaotic attractors. So they are not diffeomorphic.

In the following, assume that the numbers of equilibria and subattractors for systems (7) and (8) are the same.

If systems (7) and (8) are diffeomorphic, then there would be a diffeomorphism,

$$y = h(x)\,, \tag{9}$$

such that

$$f(x) = M^{-1}(x) g(h(x))\,, \tag{10}$$

where $M(x) = dh(x)/dx$ is the Jacobian of $h(x)$ evaluated at x. Let x_0 and $y_0 = h(x_0)$ be such equilibria and let $A(x_0)$ and $B(y_0)$ denote the corresponding Jacobians. Then, differentiating (10) would yield

$$A(x_0) = M^{-1}(x_0) B(y_0) M(x_0)\,. \tag{11}$$

Therefore, the characteristic polynomials for the matrices $A(x_0)$ and $B(y_0)$ should coincide.

However, because the eigenvalues of the corresponding Jacobians are not equivalent, systems (7) and (8) are not diffeomorphic.

Furthermore, chaotic system (1) is not topologically equivalent with any known three-dimensional quadratic autonomous chaotic system. Actually, if the numbers of equilibria or subattractors for systems (7) and (8) are not the same, then they are not topologically equivalent. Similarly, we can verify the topological equivalent by rather tedious algebraical operation and is omitted here. The proof is thus completed. ■

4.2. *Equilibria and bifurcations*

It is easily verified that if $ab > 0$ then system (6) has five equilibria:

$$S_1(0,\, 0,\, 0)$$

$$S_2\left(\sqrt{ab},\, |b|\sqrt{\frac{a}{a+b}},\, -a\sqrt{\frac{b}{a+b}}\right)$$

$$S_3\left(\sqrt{ab},\, -|b|\sqrt{\frac{a}{a+b}},\, a\sqrt{\frac{b}{a+b}}\right)$$

$$S_4\left(-\sqrt{ab},\ |b|\sqrt{\frac{a}{a+b}},\ a\sqrt{\frac{b}{a+b}}\right)$$

$$S_5\left(-\sqrt{ab},\ -|b|\sqrt{\frac{a}{a+b}},\ -a\sqrt{\frac{b}{a+b}}\right).$$

If $ab \le 0$, then system (6) has a unique equilibrium, $S_1(0,\,0,\,0)$.

Pitchfork bifurcation of the null solution at $a = 0$ (or $b = 0$) can be observed, if b (or a) is fixed but a (or b) is varied.

Moreover, any two nonzero equilibria are symmetric about one of the axes x, y, z, that is,

- S_2 and S_3, S_4 and S_5 are symmetric with respect to the x-axis.
- S_2 and S_4, S_3 and S_5 are symmetric with respect to the y-axis.
- S_2 and S_5, S_3 and S_4 are symmetric with respect to the z-axis.

It is also noticed that the origin is always a saddle point in the three-dimensional space for any nonzero real numbers a, b.

Linearization of system (6) about the null solution S_1 gives three eigenvalues: $\lambda_1 = -ab/(a+b)$, $\lambda_2 = a$, and $\lambda_3 = b$.

Next, linearizing the system about the nonzero equilibria S_2, S_3, S_4, S_5 yields the following same characteristic equation:

$$f(\lambda) = \lambda^3 - \frac{a^2+ab+b^2}{a+b}\lambda^2 - \frac{4a^2b^2}{a+b} = 0\,. \quad (12)$$

Theorem 2. *Hopf bifurcation will not appear at any equilibrium $S_i (i = 1, \ldots, 5)$ of system (6).*

Proof. Since the characteristic equation for equilibrium $S_1(0,\,0,\,0)$ has three eigenvalues: $\lambda_1 = -ab/(a+b)$, $\lambda_2 = a$, and $\lambda_3 = b$, one can see that there is no Hopf bifurcation at S_1.

For equilibria S_2, S_3, S_4, S_5, they have the same characteristic equation (12), so only the equilibrium S_2 is discussed. If Hopf bifurcation appears at equilibrium S_2, then it may be assumed that two zeros are $\lambda = \pm\omega i$ for some real ω, and the sum of the three zeros of the cubic polynomial f is

$$\lambda_1 + \lambda_2 + \lambda_3 = \frac{a^2+ab+b^2}{a+b}\,.$$

Hence, $\lambda_3 = (a^2+ab+b^2)/(a+b)$. However

$$f\left(\frac{a^2+ab+b^2}{a+b}\right) = -\frac{4a^2b^2}{a+b} = 0\,,$$

that is, $ab = 0$. This contradicts with the condition $ab > 0$. Therefore, there is no Hopf bifurcation at S_2. This completes the proof of the theorem. ■

Remarks

(1) It is quite a strange phenomenon to have no Hopf bifurcation in a three-dimensional quadratic autonomous chaotic system. All known three-dimensional quadratic autonomous chaotic systems have Hopf bifurcations at some of their equilibria, such as in the Lorenz system [Lorenz, 1963], Chen system [Chen & Ueta, 1999; Lü *et al.*, 2002g, 2002h], transition system [Lü & Chen, 2002; Lü *et al.*, 2002b], unified chaotic system [Lü *et al.*, 2002a].

(2) Since the coefficient of λ in Eq. (12) is zero, Eq. (12) does not have two conjugate imaginary roots for any parameters a, b. However, the coefficient of λ in the characteristic equation is nonzero for most known three-dimensional quadratic autonomous chaotic systems such as those just mentioned.

If system (6) is dissipative, then $a+b < 0$. Since $ab > 0$, one has $a < 0$, $b < 0$. Note that the coefficients of the cubic characteristic polynomial are all positive, so that $f(\lambda) > 0$ for all $\lambda > 0$. It is noted that instability appears ($\mathrm{Re}(\lambda) > 0$) only if there are two complex conjugate zeros of f. In fact, Eq. (12) has one negative real root and two complex conjugate roots with positive real part.

Consider Eq. (12). Denote

$$A = -\frac{a^2+ab+b^2}{a+b} > 0, \quad B = 0, \quad C = -\frac{4a^2b^2}{a+b} > 0$$

and assume that $\lambda = -(A/3) + \Lambda$, then, Eq. (12) becomes

$$f(\Lambda) = \Lambda^3 + P\Lambda + Q\,,$$

where

$$P = -\frac{A^2}{3} + B = -\frac{A^2}{3}$$

and

$$Q = \frac{2A^3}{27} - \frac{AB}{3} + C = \frac{2A^3}{27} + C\,.$$

This third-order polynomial in Λ can be solved by using the Cardan formula, whereby one may set

$\Delta = 4P^3+27Q^2 = 27C^2+4A^3C > 0$. Consequently, Eq. (12) has a unique real eigenvalue.

$$\begin{aligned}\lambda_1 &= -\frac{A}{3} + \Lambda \\ &= -\frac{A}{3} + \frac{1}{6} - \sqrt[3]{-108Q + 12\sqrt{12P^3 + 81Q^2}} \\ &\quad - \frac{2P}{\sqrt[3]{-108Q + 12\sqrt{12P^3 + 81Q^2}}}, \end{aligned} \tag{13}$$

along with two complex conjugate eigenvalues,

$$\begin{aligned}\lambda_{2,3} &= -\frac{A}{3} - \frac{1}{12}\sqrt[3]{-108Q + 12\sqrt{12P^3 + 81Q^2}} \\ &\quad + \frac{P}{\sqrt[3]{-108Q + 12\sqrt{12P^3 + 81Q^2}}} \\ &\quad \pm \frac{\sqrt{3}}{2} i \left(\frac{1}{6}\sqrt[3]{-108Q + 12\sqrt{12P^3 + 81Q^2}} \right. \\ &\quad \left. + \frac{2P}{\sqrt[3]{-108Q + 12\sqrt{12P^3 + 81Q^2}}} \right), \end{aligned} \tag{14}$$

when $a < 0$, $b < 0$, $\lambda_1 < 0$ and $\mathbf{Re}(\lambda_{2,3}) > 0$. Therefore, the equilibria $S_i (i = 1, \ldots, 5)$ are unstable and, in fact, they are saddle-foci.

4.3. *Dynamical structure of the new chaotic system*

The dynamical behaviors of system (6) are further investigated by means of Poincaré mapping, parameter phase portraits, and calculated Lyapunov exponents and power spectra.

Figure 3 shows some dynamical behaviors in the a–b plane for system (6). In this figure, generally there exist three divisions in the plane, that is, limit cycles, a chaotic region, and then limit cycles again. The parameter values that detach these regions are calculated with Lyapunov exponents and then analyzing the resulting phase portraits, Poincaré mapping and power spectra.

Region A is a limit cycle region, where all orbits converge to some limit cycles. Furthermore, when the initial point (x_0, y_0, z_0) is above the plane $z = 0$, that is, for $z_0 > 0$, all trajectories converge to the upper limit cycle as shown in Fig. 4(a). However, when the initial point (x_0, y_0, z_0) is below the plane $z = 0$, that is, when $z_0 < 0$, all orbits converge to the down limit cycle displayed in Fig. 4(a).

Region B has the onset of chaos, and it is a region with period-doubling bifurcations. Similarly, if $z_0 > 0$ then the period-doubling bifurcations for the upper-attractor will appear, as displayed in Fig. 4(b); if $z_0 < 0$, then the period-doubling bifurcations for the lower-attractor will appear, as shown in Fig. 4(b). The forming procedure for the

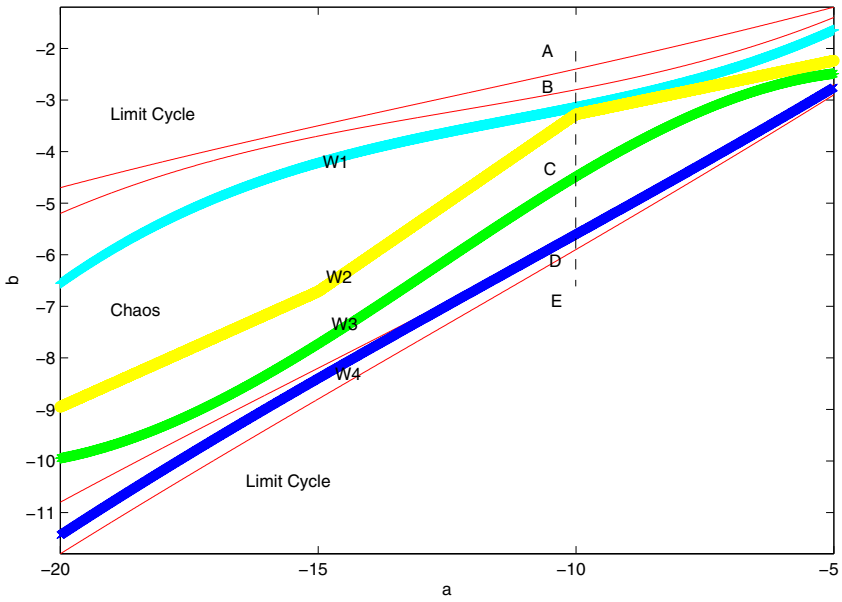

Fig. 3. Dynamical behaviors of system (6).

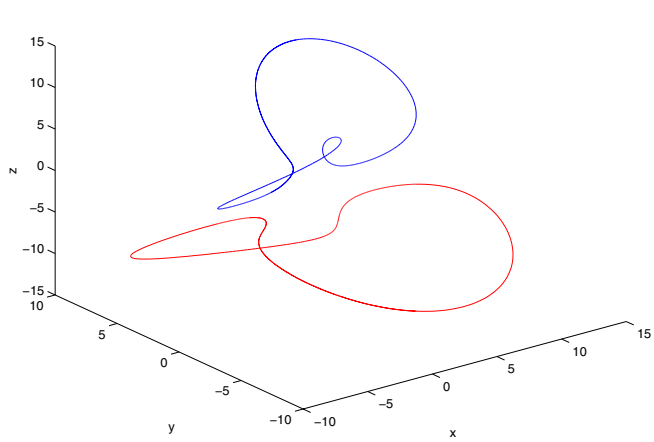

(a)

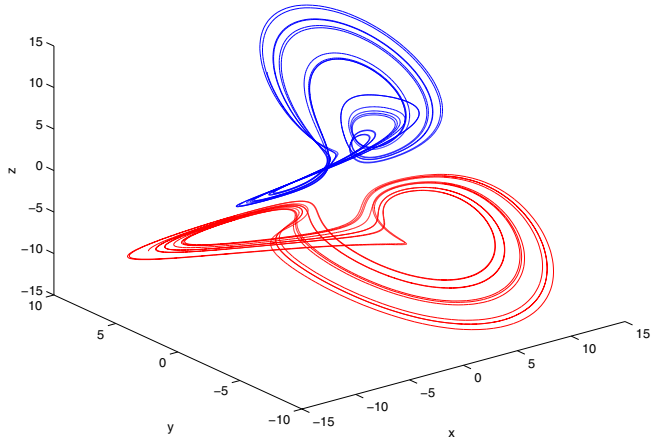

(b)

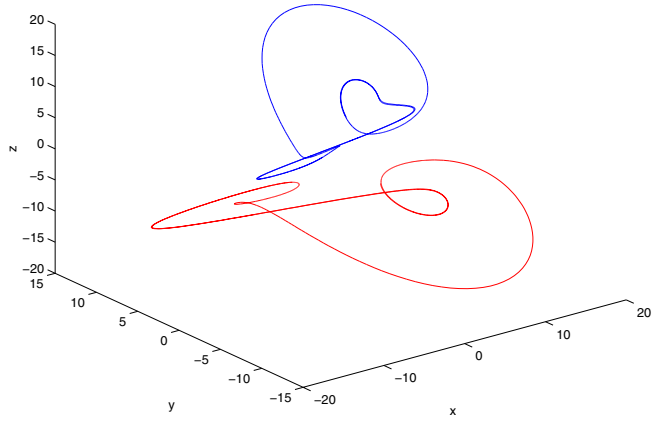

(c)

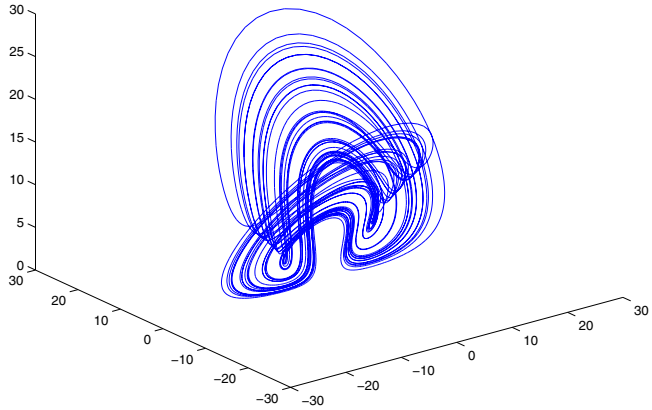

(d)

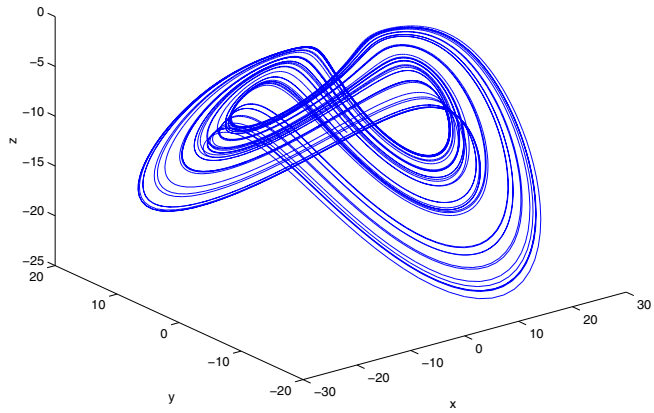

(e)

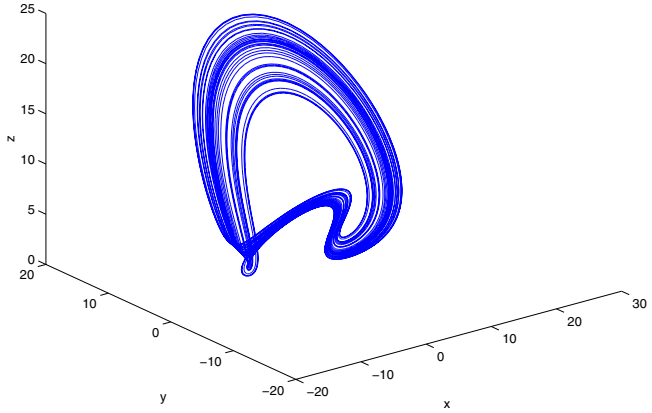

(f)

Fig. 4. Phase portraits of the stable attractors. (a) $b = -2.3$, (b) $b = -2.5$, (c) $b = -4.485$, (d) $b = -5.5$ (1, 1, 1), (e) $b = -5.5$ (1, 1, -1), (f) $b = -5.7$ (1, 1, 1), (g) $b = -5.7$ (1, 1, -1), (h) $b = -6$.

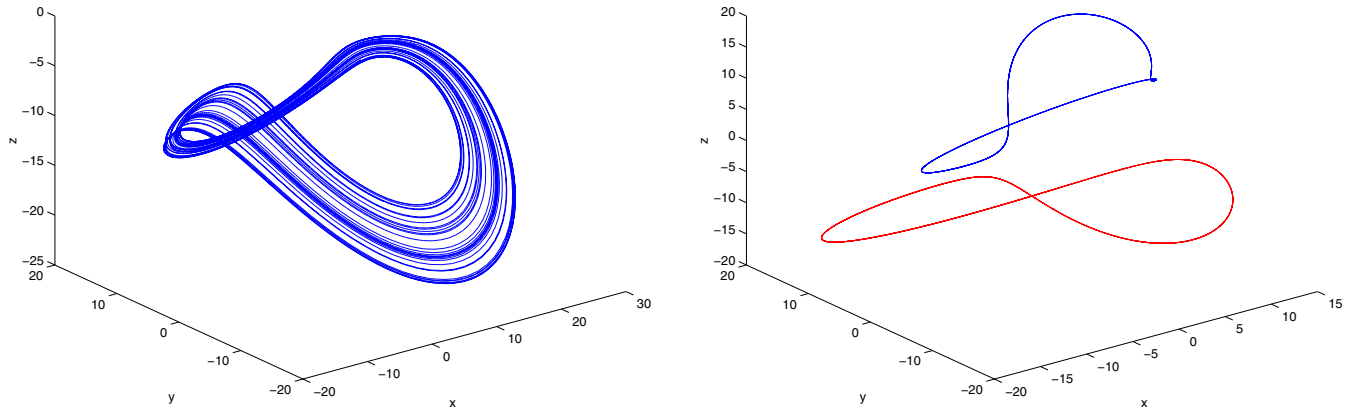

(g) (h)

Fig. 4. (*Continued*)

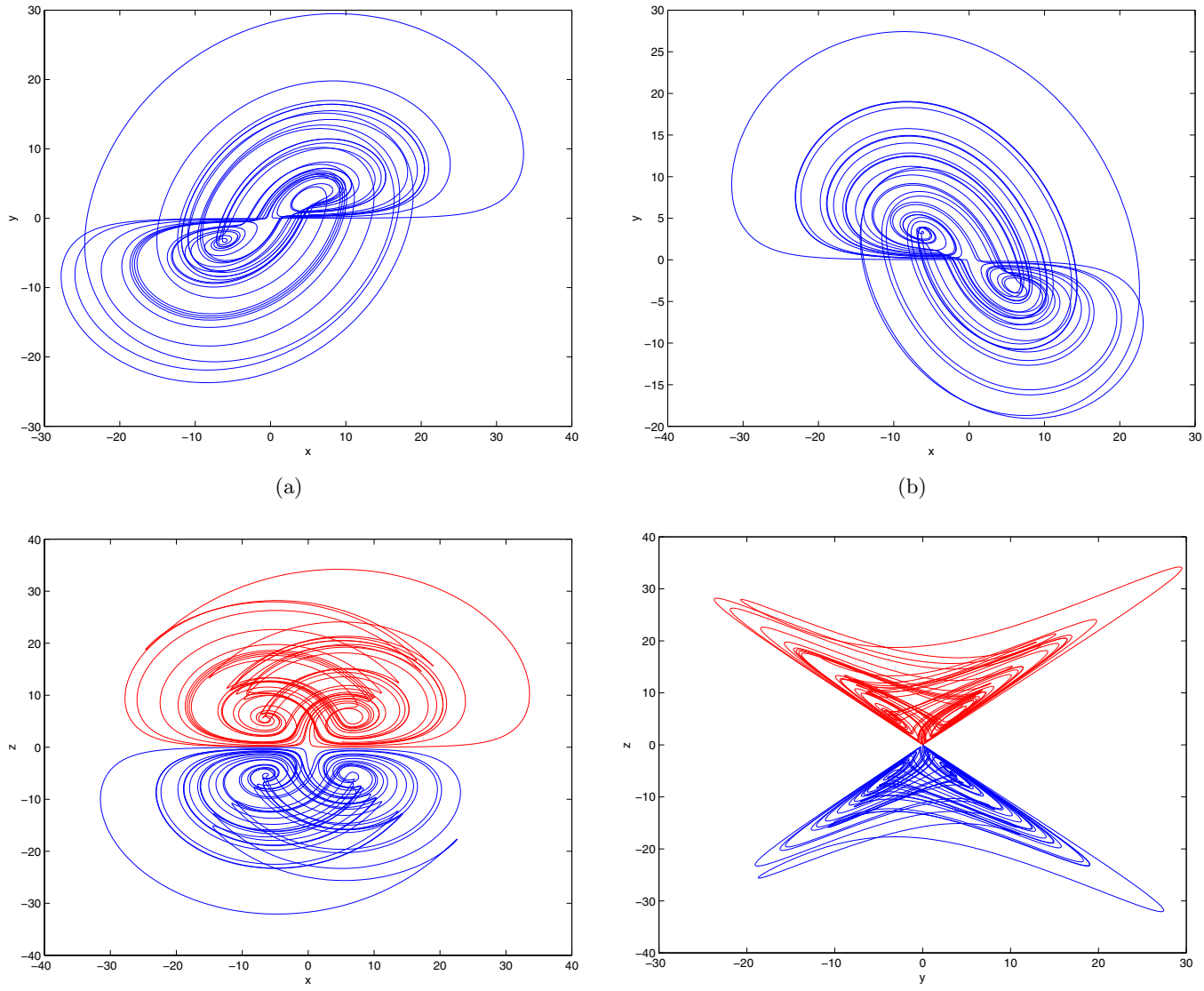

(a) (b)

(c) (d)

Fig. 5. Various projections of the upper-attractor and lower-attractor shown in Fig. 2. (a) x–y (upper-attractor), (b) x–y (lower-attractor), (c) x–z, (d) y–z.

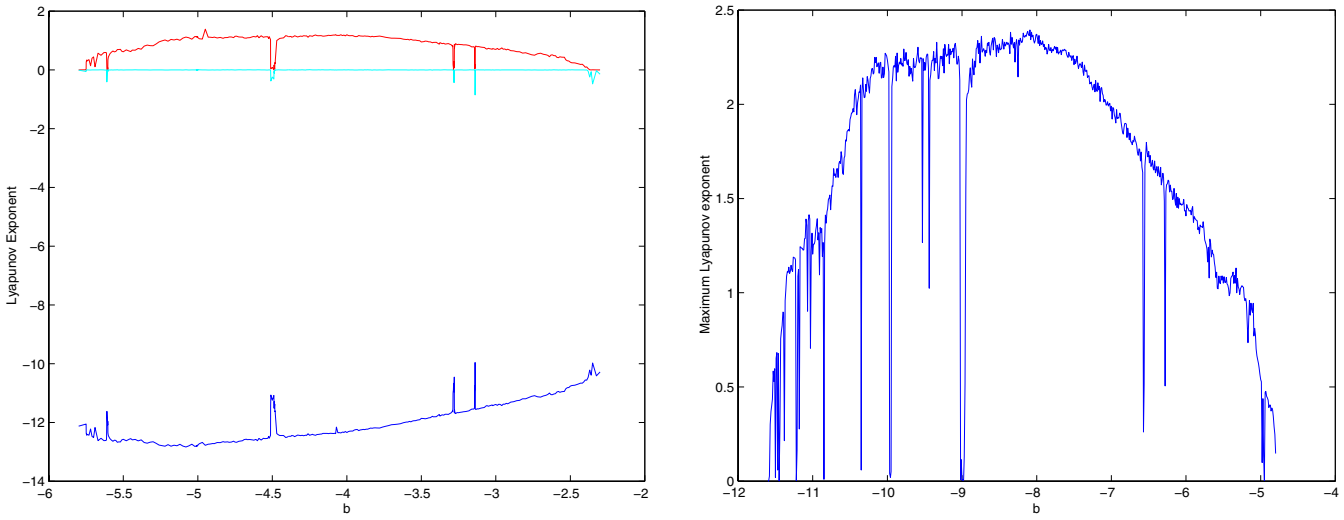

(a) (b)

Fig. 6. The Lyapunov exponent spectra. (a) $a = -10$, (b) $a = -20$.

upper-attractor and lower-attractor can be clearly seen from Fig. 4(b).

Region C is a chaotic region, where there are three typical periodic windows denoted by W_1, W_2, W_3. Figure 4(c) shows the typical periodic orbits in the periodic window W_3. When $z_0 > 0$, all orbits will converge to the upper periodic orbit, while if $z_0 < 0$, then they tend to the down periodic orbit. In region C, if $z_0 > 0$ then the system displays a chaotic attractor above the plane $z = 0$, as shown in Fig. 4(d); if $z_0 < 0$ then the system shows another chaotic attractor below the plane $z = 0$, as displayed in Fig. 4(e).

Region D is a region with period-doubling bifurcations. When $z_0 > 0$, the period-doubling bifurcations for the upper-attractor are shown in Fig. 4(f); when $z_0 < 0$, the period-doubling bifurcations for the lower-attractor are displayed in Fig. 4(g). From Figs. 4(f) and 4(g), one can clearly see the forming mechanisms for the upper-attractor and lower-attractor. In addition, there is a periodic window W_4 in Region D.

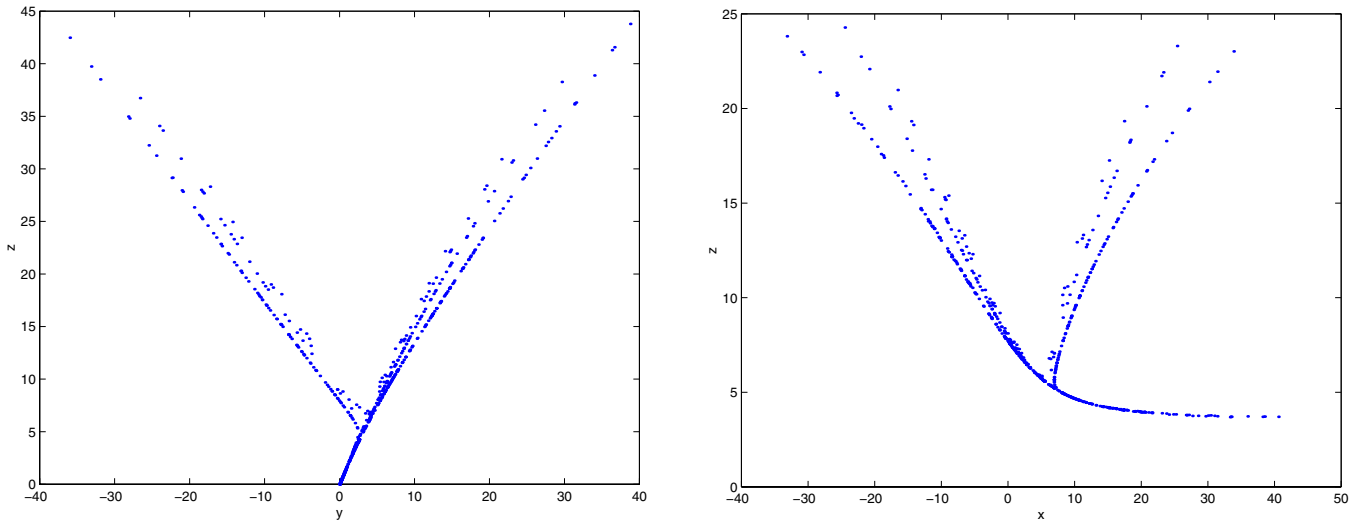

(a) (b)

Fig. 7. Poincaré mappings. (a) $x = 2\sqrt{10}$, (b) $y = (4/7)\sqrt{35}$, (c) $z = (10/7)\sqrt{14}$, (d) $y = 0$.

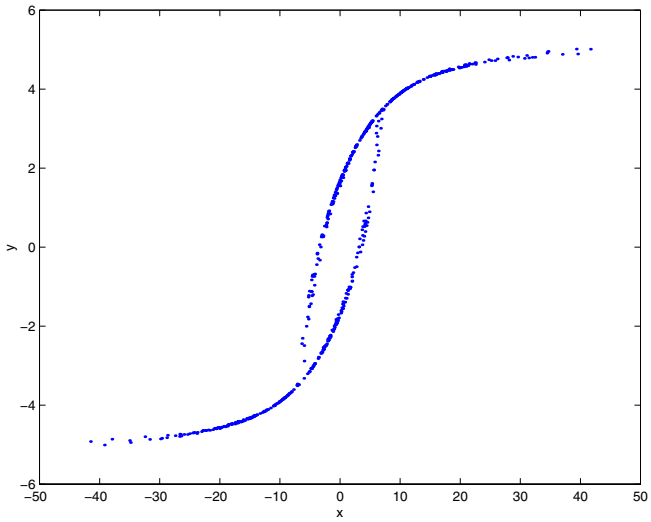

(c)

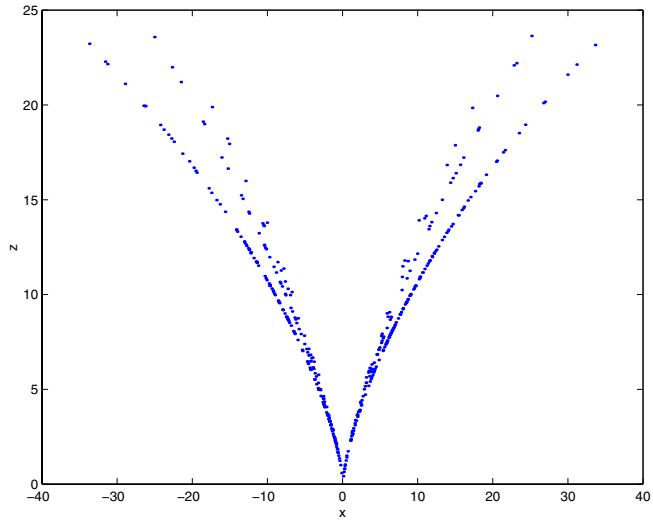

(d)

Fig. 7. (*Continued*)

Region E is a limit cyclic region, where all orbits converge to one of the two limit cycles, as shown in Fig. 4(h). Moreover, the trajectories converge to the upper limit cycle for $z_0 > 0$, but to the lower limit cycle for $z_0 < 0$.

Obviously, there are two period-doubling bifurcation regions, B, D, in the above-described diagram, that is, there are two routes to chaos. Especially, these two routes are typical of period-doubling bifurcations to chaos. However, they are different from many known three-dimensional quadratic autonomous chaotic systems such as the Lorenz system. The Lorenz system has two routes to chaos, but only one route via the typical period-doubling bifurcations. Moreover, the coexistence of period-doubling bifurcations and intermittency is observed in Regions B and D here. Also, there are two limit cycle regions, A, E, in the diagram. Most of known three-dimensional quadratic autonomous chaotic systems such as the Lorenz and Chen systems have only one limit cycle region together with a sink region.

Notice also that in the diagram there are four typical periodic windows, W_1, W_2, W_3, W_4, marked by cyan, yellow, green, and blue, respectively, in Fig. 3. These periodic windows play an important role in the evolution of the dynamical behaviors. Figure 4 displays the abundant and complex phenomena of system (6). It is very interesting to observe that the maximum periodic window W_2 is located inside the chaotic regions.

In order to investigate detailed dynamical behaviors for system (6), several situations are further analyzed in the following.

Table 1. A summary of the parameter range for behaviors of system (6) as determined by both theoretical analysis and numerical computation ($a = -10$).

For $-2.34 < b < 0$, there are limit cycles;
For $-2.8 \leq b \leq -2.34$, there are period-doubling bifurcations;
For $b = -2.34$, there is a period-2 bifurcation point;
For $b = -2.37$, there is a period-4 bifurcation point;
For $-5.6 \leq b < -2.8$, the system has two 2-scroll chaotic attractors, and one is above the plane $z = 0$ while the other is below the plane $z = 0$;
For $-3.141 \leq b \leq -3.139$, there is a periodic window;
For $-3.285 \leq b \leq -3.278$, there is a periodic window;
For $-4.511 \leq b \leq -4.484$, there is a periodic window;
For $-5.93 \leq b < -5.6$, there are period-doubling bifurcations;
For $-5.611 \leq b \leq -5.604$, there is a periodic window;
For $b = -5.82$, there is a period-4 bifurcation point;
For $b = -5.93$, there is a period-2 bifurcation point;
For $b < -5.93$, there are two period-1 limit cycles, and one is above the plane $z = 0$ whilst the other is below the plane $z = 0$.

Case 1 ($a = -10$). When $a = -10$, $b = -4$, system (6) has five equilibria: $S_1\,(0, 0, 0)$, $S_2(2\sqrt{10}, (4/7)\sqrt{35}, (10/7)\sqrt{14})$, $S_3(2\sqrt{10}, (-4/7)\sqrt{35}, (-10/7)\sqrt{14})$, $S_4(-2\sqrt{10}, (4/7)\sqrt{35}, (-10/7)\sqrt{14})$, $S_5(-2\sqrt{10}, (-4/7)\sqrt{35}, (10/7)\sqrt{14})$.

The characteristic roots for S_1 are $\lambda_1 = 20/7$, $\lambda_2 = -10$, $\lambda_3 = -4$, so S_1 is a saddle point. And the characteristic roots for the other equilibria are $\lambda_1 \approx -13.6106$, $\lambda_{2,3} \approx 1.2339 \pm 5.6626i$, thus the equilibria S_2, S_3, S_4, S_5 are all saddle-foci.

Figure 5 further displays the projections of the upper-attractor and lower-attractor onto the x–y, x–z and y–z planes, respectively.

Figure 6(a) shows the corresponding Lyapunov exponents versus the varying parameter b.

Figure 7 shows the Poincaré mapping on several sections, with several sheets of the attractors visualized. It is clear that some sheets are folded.

Table 1 lists the domains of the parameter b, in which system (6) has complex dynamical behaviors.

Case 2 ($a = -20$). Figure 6(b) shows the corresponding maximum Lyapunov exponents versus the varying parameter b. There are eleven periodic windows in the Lyapunov exponent spectra:

$W_1[-4.981, -4.979]$, $W_2[-4.963, -4.946]$,
$W_3[-6.284, -6.278]$, $W_4[-6.575, -6.555]$,
$W_5[-9.022, -8.951]$, $W_6[-9.44, -9.437]$,
$W_7[-9.531, -9.529]$, $W_8[-9.97, -9.948]$,
$W_9[-10.352, -10.348]$, $W_{10}[-10.851, -10.849]$,
$W_{11}[-11.451, -11.439]$.

These periodic windows play an important role in the evolution of dynamical behaviors of system (6). Other parameter ranges for behaviors of system (6) can be similarly obtained, which are however omitted here.

5. Compound Structure of the Upper-Attractor and Lower-Attractor

It was found that the Chen attractor [Chen & Ueta, 1999] and transition attractor [Lü & Chen, 2002] both have a compound structure [Lü *et al.*, 2002c, 2002g]. That is, they can be obtained by merging together two simple attractors after performing a mirror operation. It is therefore interesting to ask if the upper-attractor and lower-attractor here also have a compound structure of two simpler attractors, respectively. This section provides a positive answer to this question.

In order to investigate the compound structures of the upper-attractor and the lower-attractor, a constant control term is added to the first equation of system (6), thereby obtaining system (1), that is,

$$\begin{cases} \dot{x} = -\dfrac{ab}{a+b}x - yz + u \\ \dot{y} = ay + xz \\ \dot{z} = bz + xy \end{cases} \tag{15}$$

where $u = c$. Assume that $a = -10$, $b = -4$. When $u = 9$, one obtains the right-attractors of the original upper-attractor and lower-attractor, and their projections on the x–z plane are shown in Figs. 8(a) and 8(b); while when $u = -9$, one has their mirror images, i.e. the two left-attractors and their projections on the x–z plane, as shown in Figs. 8(c) and 8(d). Detailed theoretical as well as numerical analysis has confirmed that the upper-attractor and lower-attractor both have a compound structure obtained by merging together the two corresponding simple left- and right-attractors via a mirror operation, respectively.

In order to study the forming mechanisms of the upper-attractor and lower-attractor, and to clarify their topological structures, the dynamical behaviors of the controlled system (15) is further studied here. It turns out to be possible to confine the chaotic dynamics to either one of the upper-attractor and lower-attractor, by changing the constant controller u, or to form two simple attractors which, when merged together, produces the upper-attractor or lower-attractor. By tuning the parameter u, as listed in Table 2, one can observe different dynamical behaviors of the controlled system.

Remarks

(1) It can be seen from Table 2 that (i) when $|u|$ is large enough, e.g. $|u| > 31.4$, system (15) has two period-1 limit cycles, as shown in Fig. 9(a); (ii) when $|u|$ decreases gradually, there appear period-doubling bifurcations [Fig. 9(b)] and then the two attractors evolve into only one half of the original upper-attractor and lower-attractor; (iii) when $|u|$ is relatively small, the two 2-scroll attractors are bounded and form two partial chaotic attractors, as displayed in Fig. 9(d); (iv) when $|u|$ is small enough, two complete 2-scroll attractors are obtained.

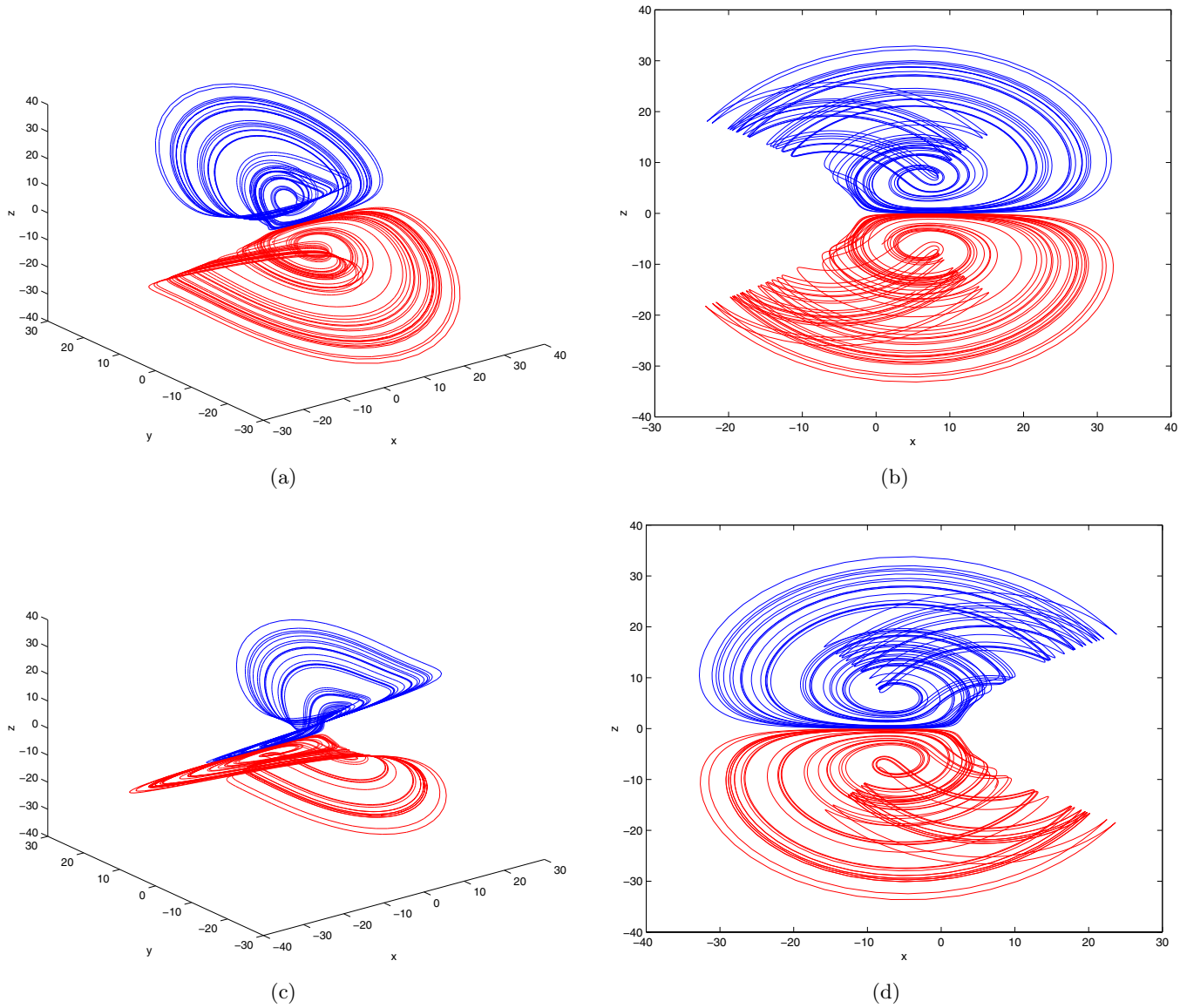

Fig. 8. The right- and left-forming attractors and their projections, for the upper-attractor and lower-attractor. (a and b) $u = 9$; (c and d) $u = -9$.

Table 2. A summary of the parameter domains for behaviors of system (15), determined by both theoretical analysis and numerical computation.

For $\|u\| > 31.4$, system (15) has two period-1 limit cycles [Fig. 9(a)];
For $21.5 \leq \|u\| \leq 31.4$, system (15) has two period-2 limit cycles;
For $19.2 \leq \|u\| < 21.5$, there are period-doubling bifurcations [Fig. 9(b)];
For $8.4 \leq \|u\| < 19.2$, system (15) has two left-attractors (or right-attractors) (Fig. 8);
For $11.9 < \|u\| \leq 14.7$, there is a big periodic window [Fig. 9(c)];
For $2.0 \leq \|u\| < 8.4$, system (15) has two partial and bounded attractors [Fig. 9(d)];
For $\|u\| < 2$, system (15) has two complete 2-scroll chaotic attractors (Fig. 2).

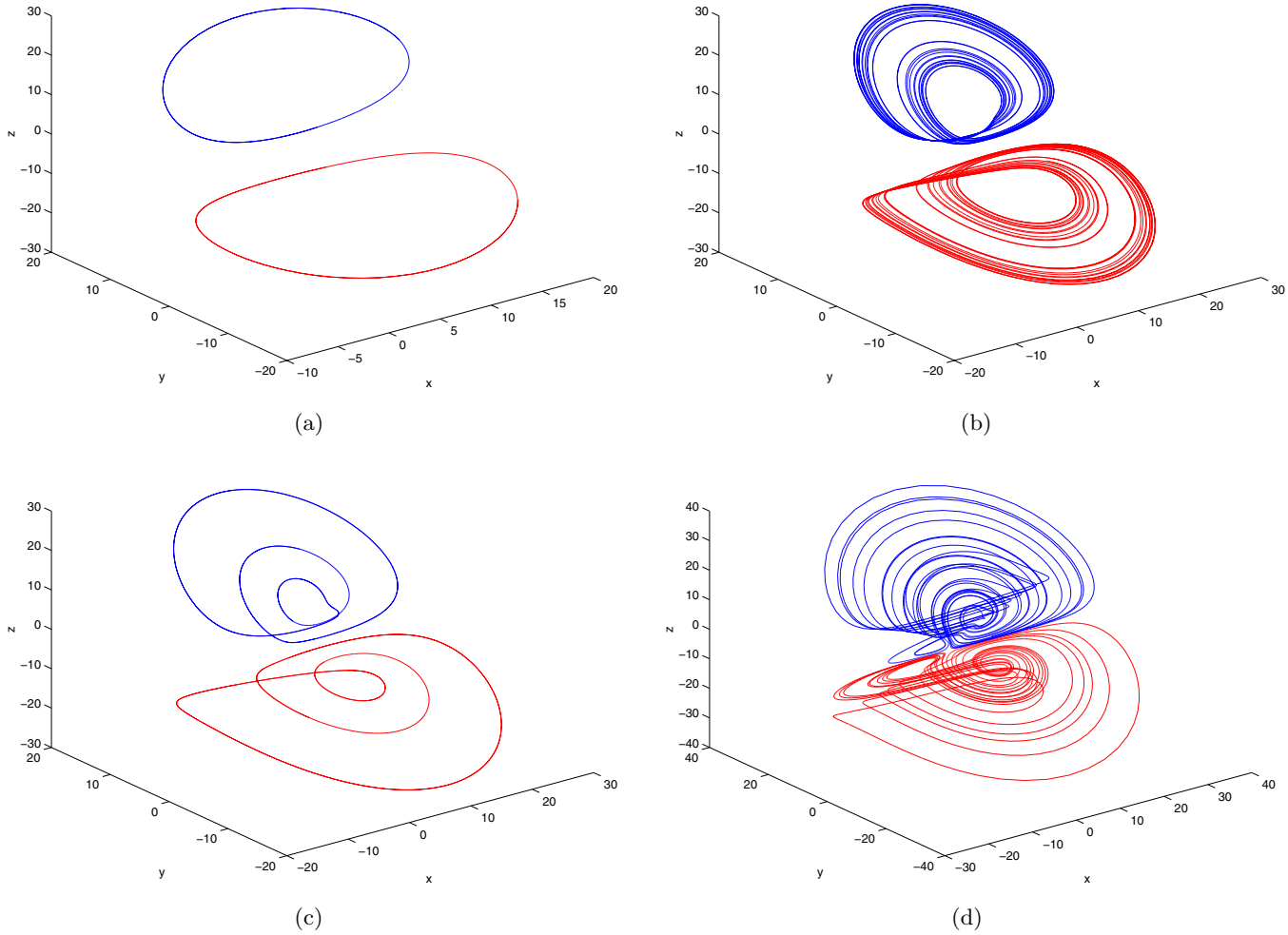

Fig. 9. Phase portraits of system (15). (a) $u = 50$, (b) $u = 19$, (c) $u = 14.7$, (d) $u = 7$.

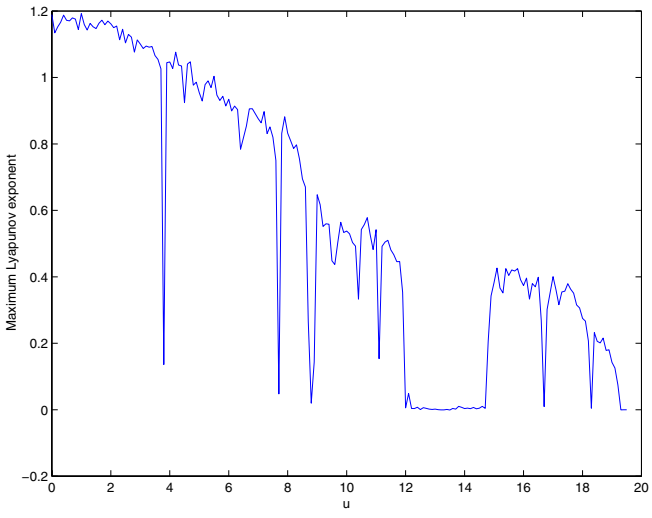

Fig. 10. The maximum Lyapunov exponent spectrum for the controlled system (15). ($a = -10$, $b = -4$, initial value (1, 1, 1).)

(2) From Figs. 9(a)–9(d), one can see that the two 2-scroll attractors — upper-attractor and lower-attractor — both have a compound structure, composed of two simple attractors respectively, and each emerges from some simple limit cycles [Fig. 9(c)]. Furthermore, the forming attractors of the upper-attractor and lower-attractor are obtained simultaneously by tuning the simple controller u.

(3) There are two big periodic windows, [11.9, 14.7] and $[-14.7, -11.9]$, in system (15), which play a key role in the forming of the two left-attractors or right-attractors.

(4) $u = \pm 31.4$ are the period-2 bifurcation points and $u = \pm 21.5$ are the period-4 bifurcation points.

(5) The controller u can change the topological structures (shapes) of the original chaotic attractors, rather than their qualitative

properties. Therefore, the controller is used here to provide a better view of the topological structures of the system is chaotic attractors.

According to Table 2, one can see that the controlled system (15) is chaotic for $|u| \leq 19.2$. Figure 10 displays the maximum Lyapunov exponent spectrum of system (15) for $0 \leq u \leq 19.2$. It can be clearly seen that there are seven periodic windows in Fig. 15: W_1 (3.79, 3.81), W_2 (7.64, 7.71), W_3 [8.78, 8.91], W_4 [11.1, 11.13], W_5 [11.93, 14.77], W_6 [16.67, 16.78], W_7 [18.25, 18.34]. These periodic windows play a key role in the evolution of the dynamics for the controlled system (15).

It is known that the number of system equilibria and their stabilities are very important for the emergence of chaos. In the following, consider the equilibria of system (15).

Theorem 3

(i) *If* $u \geq (-ab/(a+b))\sqrt{ab}$, *then system* (15) *has three equilibria*:

$$S_1'\left(\frac{a+b}{ab}u, 0, 0\right)$$

$$S_2'\left(\sqrt{ab}, \sqrt{b\left(\frac{ab}{a+b}-\frac{u}{\sqrt{ab}}\right)}, \sqrt{a\left(\frac{ab}{a+b}-\frac{u}{\sqrt{ab}}\right)}\right)$$

$$S_3'\left(\sqrt{ab}, -\sqrt{b\left(\frac{ab}{a+b}-\frac{u}{\sqrt{ab}}\right)}, -\sqrt{a\left(\frac{ab}{a+b}-\frac{u}{\sqrt{ab}}\right)}\right).$$

(ii) *If* $u \leq (ab/(a+b))\sqrt{ab}$, *then system* (15) *has three equilibria*:

$$S_1'\left(\frac{a+b}{ab}u, 0, 0\right)$$

$$S_4'\left(-\sqrt{ab}, -\sqrt{b\left(\frac{ab}{a+b}+\frac{u}{\sqrt{ab}}\right)}, \sqrt{a\left(\frac{ab}{a+b}+\frac{u}{\sqrt{ab}}\right)}\right)$$

$$S_5'\left(-\sqrt{ab}, \sqrt{b\left(\frac{ab}{a+b}+\frac{u}{\sqrt{ab}}\right)}, -\sqrt{a\left(\frac{ab}{a+b}+\frac{u}{\sqrt{ab}}\right)}\right).$$

(iii) *If* $|u| < (-ab/(a+b))\sqrt{ab}$, *then system* (15) *has five equilibria*: $S_1'(((a+b)/ab)u, 0, 0)$, S_2', S_3', S_4', S_5'.

Let $a = -10$, $b = -4$. Then the equilibria of the controlled system (15) are obtained as follows:

When $u \geq (-40/7)\sqrt{10} \approx 18.0702$, system (15) has three equilibria:

$$S_1'\left(-\frac{7u}{20}, 0, 0\right),$$

$$S_2'\left(2\sqrt{10}, \sqrt{\frac{80}{7}+\frac{\sqrt{10}}{5}u}, \sqrt{\frac{200}{7}+\frac{\sqrt{10}}{2}u}\right),$$

$$S_3'\left(2\sqrt{10}, -\sqrt{\frac{80}{7}+\frac{\sqrt{10}}{5}u}, -\sqrt{\frac{200}{7}+\frac{\sqrt{10}}{2}u}\right);$$

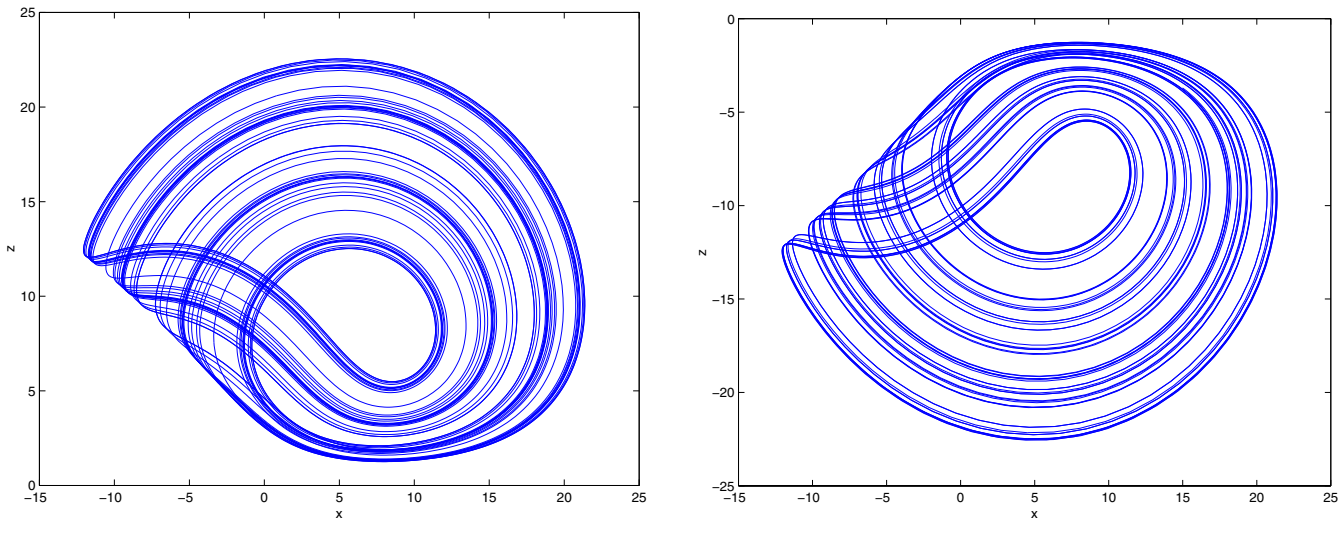

(a) (b)

Fig. 11. The x–z plane projections of the two chaotic attractors of system (15). (a) Initial value (x_0, y_0, z_0) $(z_0 > 0)$; (b) initial value (x_0, y_0, z_0) $(z_0 < 0)$; $(a = -10, b = -4, u = 18.1)$.

when $u \le (-40/7)\sqrt{10}$, the system (15) has three equilibria:

$$S_1'\left(-\frac{7u}{20},\, 0,\, 0\right),$$

$$S_4'\left(-2\sqrt{10},\, -\sqrt{\frac{80}{7}-\frac{\sqrt{10}}{5}u},\, \sqrt{\frac{200}{7}-\frac{\sqrt{10}}{2}u}\right),$$

$$S_5'\left(-2\sqrt{10},\, \sqrt{\frac{80}{7}-\frac{\sqrt{10}}{5}u},\quad -\sqrt{\frac{200}{7}+\frac{\sqrt{10}}{2}u}\right);$$

when $|u| < (-40/7)\sqrt{10}$, system (15) has five equilibria:

S_1', S_2', S_3', S_4', S_5'. According to Table 2, system (15) also has two 2-scroll chaotic attractors for $(40/7)\sqrt{10} \le |u| \le 19.2$. However, for $|u| \ge (40/7)\sqrt{10}$, system (15) has only three equilibria. This is quite a strange phenomenon in three-dimensional quadratic chaotic systems. Assume that $u = 18.1 > (40/7)\sqrt{10}$, then system (15) has three equilibria: $S_1'(-6.335,\, 0,\, 0)$, $S_2'(6.3246,\, 4.7829,\, 7.5624)$, $S_3'(6.3246,\, -4.7829,\, -7.5624)$. Figure 11 shows the x–z plane projections of the two chaotic attractors for system (15).

6. Connecting the Upper-Attractor and Lower-Attractor

As mentioned, system (6) has five equilibria:

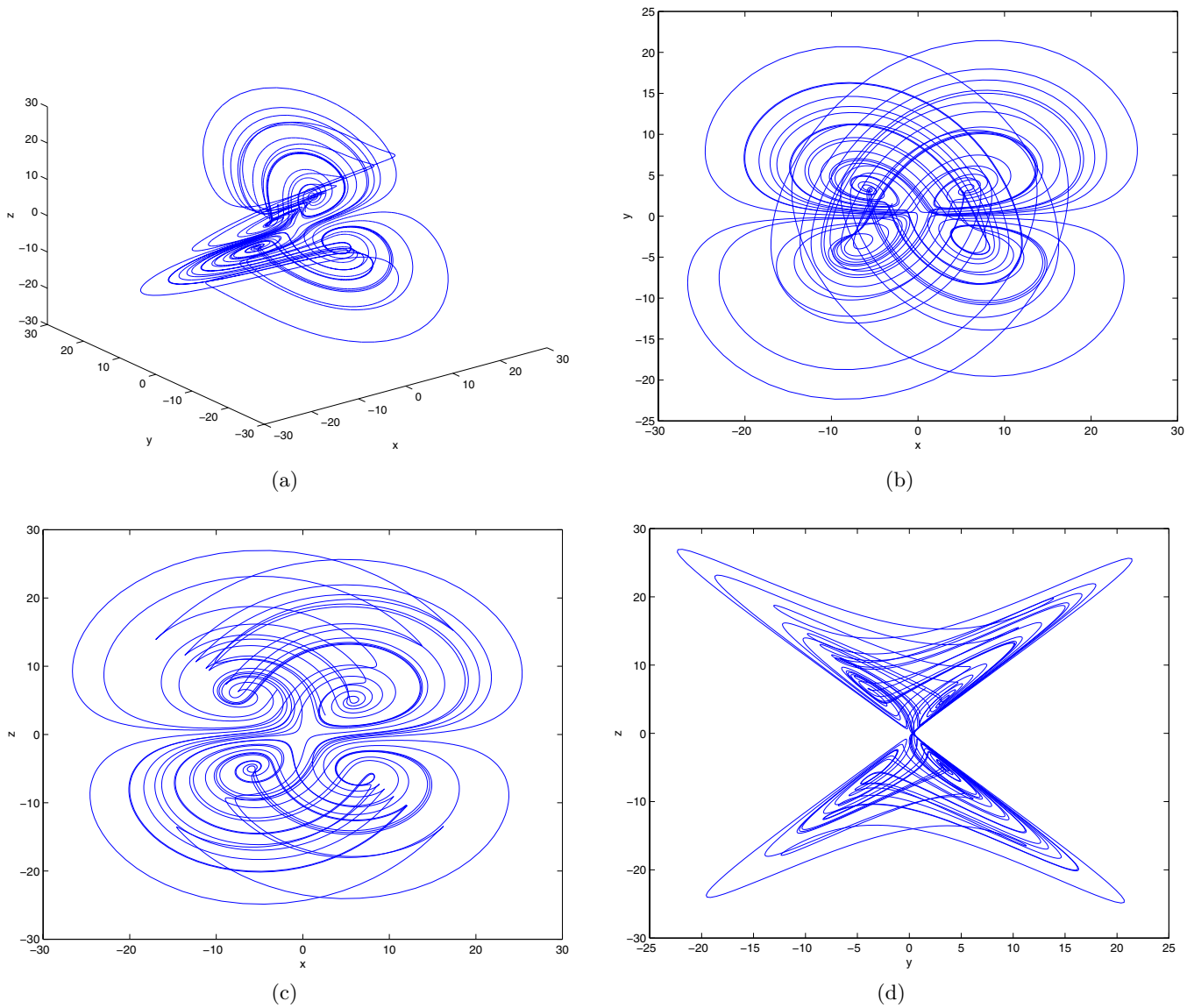

Fig. 12. The 4-scroll chaotic attractor of system (16) and its projections on various planes. (a) 3D phase portrait, (b) x–y plane projection, (c) x–z plane projection, (d) y–z plane projection. ($a = -10$, $b = -4$, $v = 5$.)

S_1, S_2, S_3, S_4, S_5, in which S_2, S_3 are above the plane $z = 0$ while S_4, S_5 are below this plane. Furthermore, there is a close correlation between the equilibria S_1, S_2, S_3 and the upper-attractor. Also, there is a close correlation between the equilibria S_1, S_4, S_5 and the lower-attractor.

Especially, the upper-attractor and lower-attractor are symmetric. It is therefore interesting to ask if there is a simple controller that can connect the upper-attractor and lower-attractor. This section gives a positive answer to this question. In fact, a constant controller works well and can

Table 3. A summary of the parameter intervals for behaviors of system (16), determined by both theoretical analysis and numerical computation.

For $\|u\| > 26.0$, the trajectories of system (16) converge to one of the two points [Fig. 13(a)];
For $24.1 \leq \|u\| \leq 26.0$, the trajectories of system (16) converge to one of the two limit cycles — upper-limit cycle and lower-limit cycle [Fig. 13(b)];
For $23.1 \leq \|u\| < 24.1$, the trajectories of system (16) converge to a limit cycle [Fig. 13(c)];
For $0.7 \leq \|u\| < 23.1$, the system (16) has a 4-scroll chaotic attractor (Fig. 12);
For $11.70 \leq \|u\| \leq 12.31$, there is a periodic window [Fig. 13(d)];
For $\|u\| < 0.7$, system (16) has two 2-scroll attractors (Fig. 2).

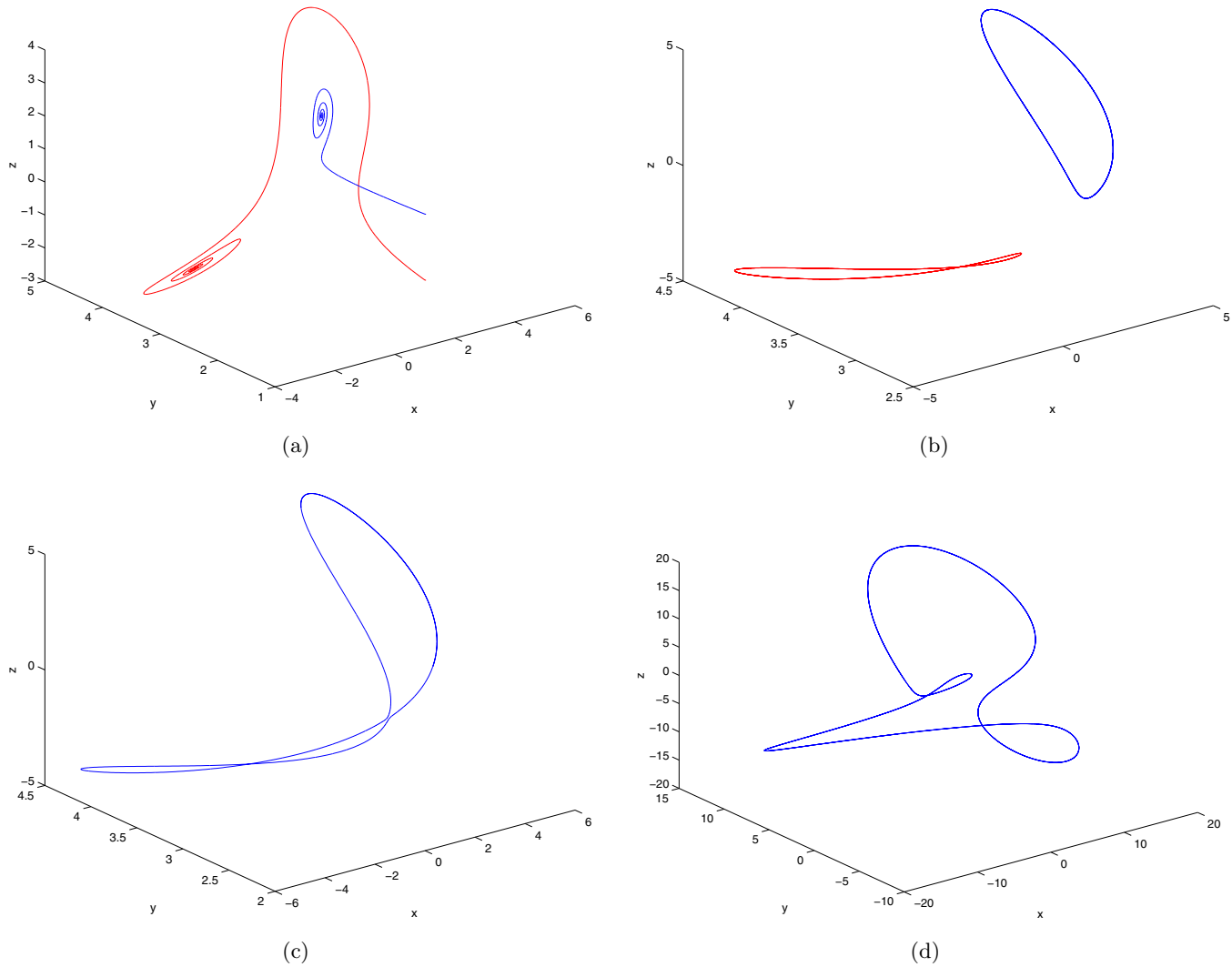

Fig. 13. Phase portraits of system (16). (a) $v = 30$, (b) $v = 25$, (c) $v = 24$, (d) $v = 12$. ($a = -10$, $b = -4$.)

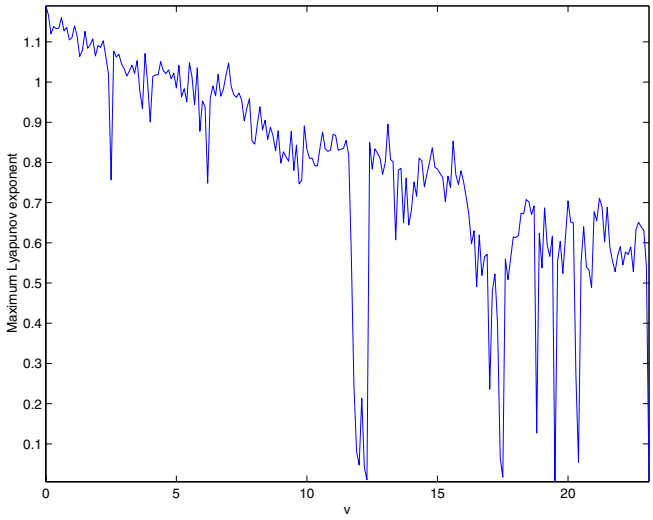

Fig. 14. The maximum Lyapunov exponent spectrum for the controlled system (16). ($a = -10$, $b = -4$, initial value (1, 1, 1).)

connect the upper-attractor and lower-attractor to form a 4-scroll chaotic attractor.

In order to connect the upper-attractor and lower-attractor, a simple constant controller v is added to the second equation of system (6), giving

$$\begin{cases} \dot{x} = -\dfrac{ab}{a+b}x - yz \\ \dot{y} = ay + xz + v \\ \dot{z} = bz + xy \end{cases} \tag{16}$$

Let $a = -10$, $b = -4$. When $v = 5$, system (16) displays a 4-scroll chaotic attractor, as shown in Fig. 12.

In order to study the forming mechanism of the 4-scroll chaotic attractor and clarify its topological structure, the dynamical behaviors of the controlled system (16) are further investigated here. By varying the control parameter v, as listed in Table 3, one can obtain different dynamical behaviors.

Remarks

(1) One can see from Table 3 that (i) when $|v|$ is large enough, e.g. $|v| > 26$, the trajectories of system (16) converge to one of the two points, as shown in Fig. 13(a); (ii) when $|v|$ decreases gradually, there appear two limit cycles — upper-limit cycle and lower-limit cycle [Fig. 13(b)], and then the two limit cycles merge into one limit cycle, as displayed in Fig. 13(c); (iii) when $|v|$ is relatively small, the two 2-scroll attractors — upper-attractor and lower-attractor — are connected and form a 4-scroll chaotic attractor, as shown in Fig. 12; (iv) when $|v|$ is small enough, system (16) has two 2-scroll attractors.

(2) There are two big periodic windows, [11.70, 12.31] and [−12.31, −11.70], in system (16), which play an important role in forming the 4-scroll chaotic attractor.

(3) From Table 3, one can see that the dynamical behavior of the controlled system (16) is very complicated.

Figure 14 displays the maximum Lyapunov exponent spectrum of system (16) for $0 \le u \le 23.1$. It is clear that there are seven periodic windows in Fig. 14: $W_1(2.51, 2.53)$, $W_2[11.70, 12.31]$, $W_3(16.96, 16.99)$, $W_4[17.33, 17.57]$, $W_5[18.79, 18.86]$, $W_6[19.49, 19.55]$, $W_7[20.31, 20.42]$. These periodic windows play a key role in the evolution of the complex dynamics for the controlled system (16).

To find the equilibria of system (16), let $dx/dt = dy/dt = dz/dt = 0$.

Theorem 4

(*i*) *If* $v \ge ab\sqrt{a/(a+b)}$, *then system* (*16*) *has three equilibria*:

$$S_1''\left(0, -\frac{v}{a}, 0\right)$$

$$S_2''\left(-\sqrt{ab + v\sqrt{\frac{a+b}{a}}},\ \ b\sqrt{\frac{a}{a+b}},\ \sqrt{\frac{a}{a+b}\left(ab + v\sqrt{\frac{a+b}{a}}\right)}\right)$$

$$S_3''\left(\sqrt{ab + v\sqrt{\frac{a+b}{a}}},\ \ b\sqrt{\frac{a}{a+b}},\ -\sqrt{\frac{a}{a+b}\left(ab + v\sqrt{\frac{a+b}{a}}\right)}\right);$$

(*ii*) *If* $v \le -ab\sqrt{a/(a+b)}$, *then system* (*16*) *has*

three equilibria:

$$S_1''\left(0, -\frac{v}{a}, 0\right)$$

$$S_4''\left(\sqrt{ab - v\sqrt{\frac{a+b}{a}}}, -b\sqrt{\frac{a}{a+b}}, \sqrt{\frac{a}{a+b}\left(ab - v\sqrt{\frac{a+b}{a}}\right)}\right)$$

$$S_5''\left(-\sqrt{ab - v\sqrt{\frac{a+b}{a}}}, -b\sqrt{\frac{a}{a+b}}, -\sqrt{\frac{a}{a+b}\left(ab - v\sqrt{\frac{a+b}{a}}\right)}\right);$$

(*iii*) If $|v| < ab\sqrt{a/(a+b)}$, then system (16) has five equilibria: $S_1''\ (0, -v/a, 0)$, S_2'', S_3'', S_4'', S_5''.

Assume that $a = -10$, $b = -4$. The equilibria of the controlled system (16) are as follows: when $v \geq 40\sqrt{5/7} \approx 33.8062$, system (16) has three equilibria:

$$S_1''\left(0, \frac{v}{10}, 0\right),$$

$$S_2''\left(-\sqrt{40 + v\sqrt{\frac{7}{5}}}, -4\sqrt{\frac{5}{7}}, \sqrt{\frac{5}{7}\left(40 + v\sqrt{\frac{7}{5}}\right)}\right),$$

$$S_3''\left(\sqrt{40 + v\sqrt{\frac{7}{5}}}, -4\sqrt{\frac{5}{7}}, -\sqrt{\frac{5}{7}\left(40 + v\sqrt{\frac{7}{5}}\right)}\right);$$

when $v \leq -40\sqrt{5/7}$, the system has three equilibria:

$$S_1''\left(0, \frac{v}{10}, 0\right),$$

$$S_4''\left(\sqrt{40 + v\sqrt{\frac{7}{5}}}, 4\sqrt{\frac{5}{7}}, \sqrt{\frac{5}{7}\left(40 + v\sqrt{\frac{7}{5}}\right)}\right),$$

$$S_5''\left(-\sqrt{40 + v\sqrt{\frac{7}{5}}}, 4\sqrt{\frac{5}{7}}, -\sqrt{\frac{5}{7}\left(40 + v\sqrt{\frac{7}{5}}\right)}\right);$$

when $|v| < 40\sqrt{5/7}$, the system has five equilibria: S_1'', S_2'', S_3'', S_4'', S_5''. According to Table 3, system (16) is chaotic for $|v| < 23.1 < 33.8062$. However, for $|v| < 33.8062$, the system has five equilibria and different dynamical behaviors, including chaos, limit cycles, and sinks.

7. Controlling in between the Upper-Attractor and Lower-Attractor

As is known now, system (6) can display two 2-scroll chaotic attractors — upper-attractor and lower-attractor. It is therefore interesting to ask what is the relationship between the upper-attractor and lower-attractor, and if the two 2-scroll chaotic attractors can be confined to either one of them via a simple constant control? This section provides a positive answer to this question.

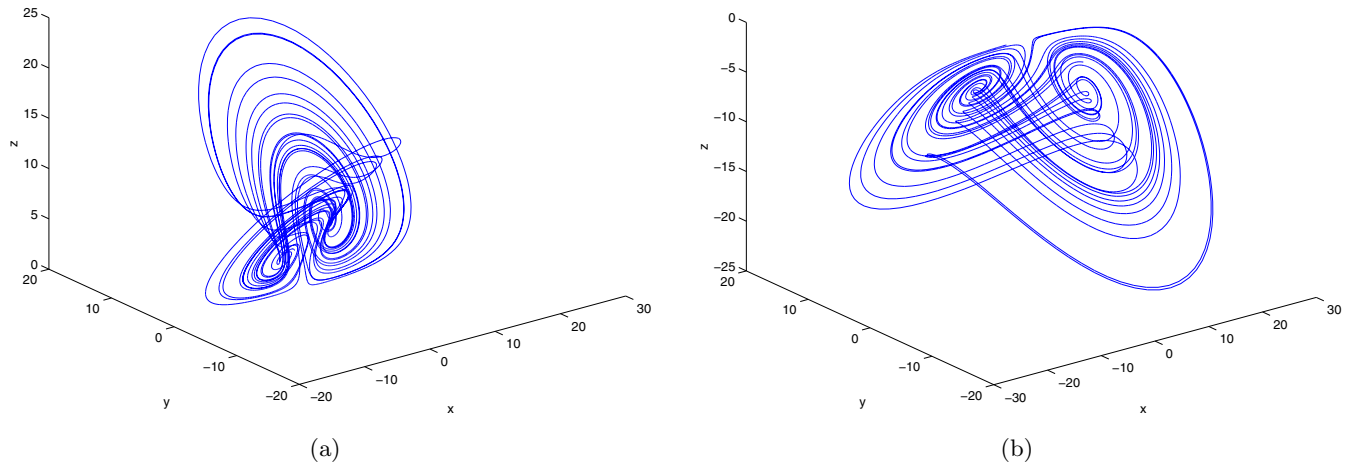

(a) (b)

Fig. 15. The 2-scroll chaotic attractors of system (17). (a) $m = 1$, (b) $m = -1$. ($a = -10$, $b = -4$.)

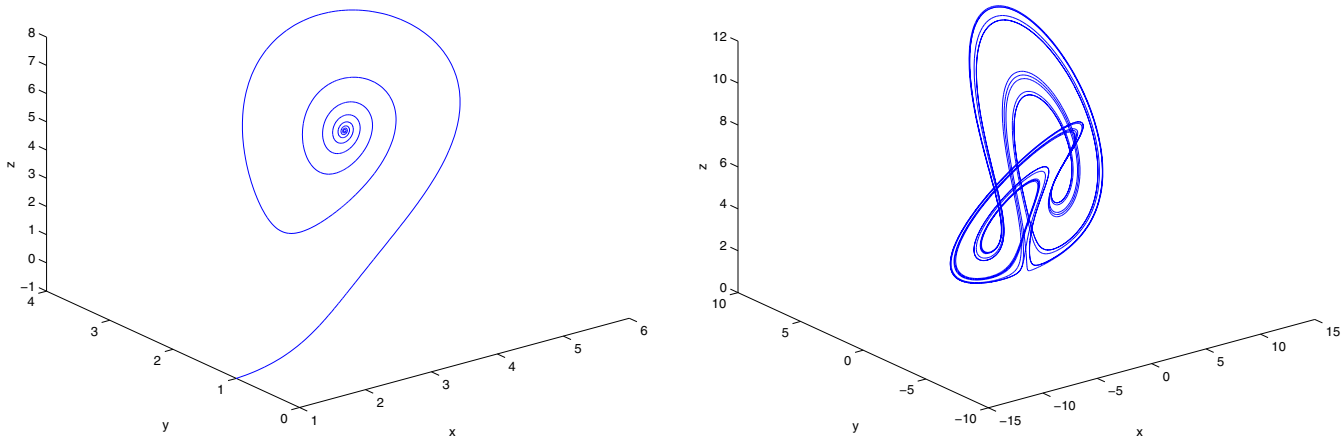

(a) (b)

Fig. 16. Phase portraits of system (17). (a) $m = 15$, (b) $m = 6.4$. ($a = -10$, $b = -4$.)

To do so, a constant controller m is added to the third equation of system (6), [Shilnikov, 1993] so as to obtain

$$\begin{cases} \dot{x} = -\dfrac{ab}{a+b}x - yz \\ \dot{y} = ay + xz \\ \dot{z} = bz + xy + m\,. \end{cases} \tag{17}$$

When $a = -10$, $b = -4$, $m = 1$, system (17) displays a 2-scroll chaotic attractor — upper-attractor — as shown in Fig. 15(a); when $m = -1$, the system shows another 2-scroll chaotic attractor — lower-attractor — as displayed in Fig. 15(b). Therefore, the original upper-attractor and lower-attractor of system (6) are confined to only one, either the upper-attractor or the lower-attractor, via a simple constant control.

In fact, system (17) establishes a kind of connection [Lü *et al.*, 2002d] between the upper-attractor and the lower-attractor. When the controller m is large, e.g. $m = 1$, system (17) only displays the upper-attractor; when the controller m is small, e.g. $m = -1$, the system only shows the lower-attractor; when $m = 0$, the system displays both.

In order to study the forming mechanism of the 2-scroll chaotic attractor and clarify its topological structure, the dynamical behaviors of the controlled system (17) are further studied here. By changing the control parameter m, as listed in Table 4, one can obtain different dynamical behaviors of the system.

Remarks

(1) It can be seen from Table 4 that (i) when $|m|$ is large enough, e.g. $|m| > 12.2$, the trajectories of system (17) converge to a point, as shown in Fig. 16(a); (ii) when $|m|$ decreases gradually, there appear period-doubling bifurcations, as displayed in Fig. 16(b); (iii) when $|m|$ is relatively small, the upper-attractor and lower-attractor are confined to a chaotic attractor, as shown in Fig. 15; (iv) when $|m|$ is small enough, system (17) also has two 2-scroll attractors.

(2) For $m > 12.2$, the trajectories of system (17) converge to a point above the plane $z = 0$, while when $m < -12.2$, to a point below the plane $z = 0$. Similarly, for $0.01 < m < 6.4$, system (17) is confined to an upper attractor whilst when $-6.4 < m < -0.01$, to a lower attractor.

(3) From Table 4, one can see that the dynamical behaviors of the controlled system (17) is relatively simple.

Table 4. A summary of the parameter domains for behaviors of system (17), determined by both theoretical analysis and numerical computation.

For $\|m\| > 12.2$, the trajectories of system (17) converge to a point [Fig. 16(a)];
For $\|m\| = 10.31$, there are two period-2 bifurcation points;
For $6.4 \le \|m\| \le 12.2$, there are period-doubling bifurcations [Fig. 16(b)];
For $0.01 < \|m\| < 6.4$, system (17) is confined to a 2-scroll attractor (Fig. 15);
For $\|m\| \le 0.01$, system (17) has two 2-scroll chaotic attractors (Fig. 2).

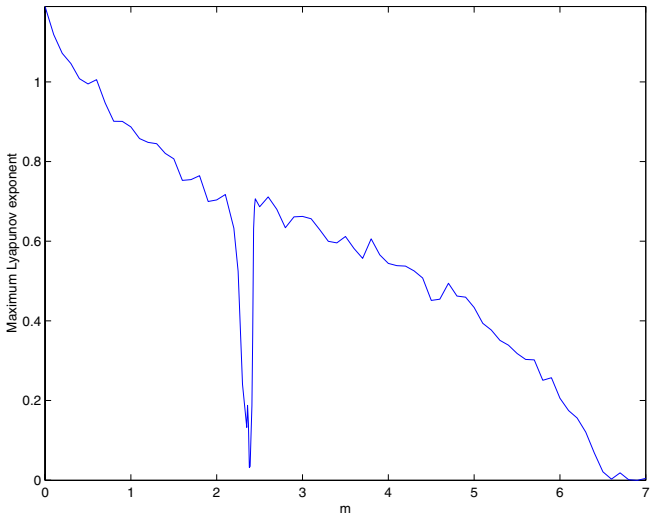

Fig. 17. The maximum Lyapunov exponent spectrum for the controlled system (17). ($a = -10$, $b = -4$, initial value (1, 1, 1).)

Figure 17 shows the maximum Lyapunov exponent spectrum of system (17) for $0 \le u \le 6.4$. Obviously, there is only one periodic window, $W[2.28, 2.42]$, in Fig. 17. However, this periodic window is very important in the evolution of the complex dynamics for the controlled system (17).

Consider the equilibria of system (17).

Theorem 5.

(i) *If* $m \ge ab\sqrt{b/(a+b)}$, *then system* (17) *has three equilibria*:

$$S_1'''\left(0,\, 0,\, -\frac{m}{b}\right)$$

$$S_2'''\left(-\sqrt{ab+m\sqrt{\frac{a+b}{b}}},\right.$$

$$\left.\sqrt{\frac{b}{a+b}\left(ab+m\sqrt{\frac{a+b}{b}}\right)},\quad a\sqrt{\frac{b}{a+b}}\right)$$

$$S_3'''\left(\sqrt{ab+m\sqrt{\frac{a+b}{b}}},\right.$$

$$\left.-\sqrt{\frac{b}{a+b}\left(ab+m\sqrt{\frac{a+b}{b}}\right)},\quad a\sqrt{\frac{b}{a+b}}\right);$$

(ii) *If* $m \le -ab\sqrt{b/(a+b)}$, *then system* (17) *has three equilibria*:

$$S_1'''\left(0,\, 0,\, -\frac{m}{b}\right)$$

$$S_4'''\left(\sqrt{ab-m\sqrt{\frac{a+b}{b}}},\right.$$

$$\left.\sqrt{\frac{b}{a+b}\left(ab-m\sqrt{\frac{a+b}{b}}\right)},\, -a\sqrt{\frac{b}{a+b}}\right)$$

$$S_5'''\left(-\sqrt{ab-m\sqrt{\frac{a+b}{b}}},\right.$$

$$\left.-\sqrt{\frac{b}{a+b}\left(ab-m\sqrt{\frac{a+b}{b}}\right)},\, -a\sqrt{\frac{b}{a+b}}\right);$$

(iii) *If* $|m| < ab\sqrt{b/(a+b)}$, *then system* (17) *has five equilibria*: $S_1'''(0,\, 0,\, -m/b)$, S_2''', S_3''', S_4''', S_5'''.

Assume that $a = -10$, $b = -4$. The equilibria of the controlled system (17) are as follows: when $m \ge 40\sqrt{2/7} \approx 21.3809$, system (17) has three equilibria:

$$S_1'''\left(0,\, 0,\, -\frac{m}{4}\right),$$

$$S_2'''\left(-\sqrt{40+m\sqrt{\frac{7}{2}}},\right.$$

$$\left.\sqrt{\frac{2}{7}\left(40+m\sqrt{\frac{7}{2}}\right)},\, -10\sqrt{\frac{2}{7}}\right),$$

$$S_3'''\left(\sqrt{40+m\sqrt{\frac{7}{2}}},\right.$$

$$\left.-\sqrt{\frac{2}{7}\left(40+m\sqrt{\frac{7}{2}}\right)},\, -10\sqrt{\frac{2}{7}}\right);$$

when $m \le -40\sqrt{2/7}$, the system has three equilibria:

$$S_1'''\left(0,\, 0,\, -\frac{m}{4}\right),$$

$$S_4'''\left(\sqrt{40-m\sqrt{\frac{7}{2}}},\, \sqrt{\frac{2}{7}\left(40-m\sqrt{\frac{7}{2}}\right)},\, 10\sqrt{\frac{2}{7}}\right),$$

$$S_5'''\left(-\sqrt{40+m\sqrt{\frac{7}{2}}},\, -\sqrt{\frac{2}{7}\left(40+m\sqrt{\frac{7}{2}}\right)},\, 10\sqrt{\frac{2}{7}}\right);$$

when $|m| < 40\sqrt{2/7}$, the system has five equilibria: S_1''', S_2''', S_3''', S_4''', S_5'''.

According to Table 4, system (17) is chaotic for $|m| \leq 6.4 < 21.3809$. Furthermore, for $|m| < 21.3809$, the system has five equilibria with different dynamical behaviors, including chaos, limit cycles and sinks.

8. The Generalized Lorenz-Like System

The Lorenz system is a very important model for studying lower-dimensional chaotic systems, especially for three-dimensional quadratic autonomous chaotic systems [Deng, 1995]. For example, Lorenz-like systems and classical dynamical equations with memory forcing were recently studied in detail [Festa *et al.*, 2002].

Vaněček and Čelikovský [1996] introduced the so-called *generalized Lorenz system*. More recently, some similar but different chaotic systems were discovered [Chen & Ueta, 1999; Lü & Chen, 2002; Chen & Lü, 2003]. In order to further investigate the dynamical behaviors of these chaotic systems and the relationships among them, Čelikovský and Chen [2002, 2003] introduced a *generalized Lorenz canonical form* of chaotic systems and a *hyperbolic-type generalized Lorenz system* and its *canonical form*, which cover a very large class of three-dimensional quadratic autonomous chaotic systems. Yet, there are still some similar systems such as the one discussed in [Rucklidge, 1992] not belonging to these generalized Lorenz systems. For this reason, the concept of generalized Lorenz system is being further extended here, giving rise to what is called *generalized Lorenz-like system* in this section.

First, recall the concept of generalized Lorenz system:

Definition 1. The nonlinear system of ordinary differential equations in $\mathbf{R}^3$ of the following form is called a generalized Lorenz system:

$$\dot{x} = \begin{pmatrix} A & 0 \\ 0 & \lambda_3 \end{pmatrix} x + x_1 \begin{pmatrix} 0 & 0 & 0 \\ 0 & 0 & -1 \\ 0 & 1 & 0 \end{pmatrix} x\,, \quad (18)$$

where $x = [x_1 \;\; x_2 \;\; x_3]^T$, $\lambda_3 \in \mathbf{R}$, and A is a 2×2 real matrix:

$$A = \begin{pmatrix} a_{11} & a_{12} \\ a_{21} & a_{22} \end{pmatrix}, \quad (19)$$

with eigenvalues λ_1, $\lambda_2 \in \mathbf{R}$ such that

$$-\lambda_2 > \lambda_1 > -\lambda_3 > 0\,. \quad (20)$$

Moreover, the generalized Lorenz system is said to be nontrivial if it has at least one solution that goes neither to zero nor to infinity or a limit cycle.

The following result can be found in [Čelikovský & Chen, 2002].

Lemma 1. *For the nontrivial generalized Lorenz system (18)–(20), there exists a nonsingular linear change of coordinates, $z = Tx$, which takes (18) into the following generalized canonical form*:

$$\dot{z} = \begin{pmatrix} \lambda_1 & 0 & 0 \\ 0 & \lambda_2 & 0 \\ 0 & 0 & \lambda_3 \end{pmatrix} z + (1, -1, 0) z \begin{pmatrix} 0 & 0 & -1 \\ 0 & 0 & -1 \\ 1 & \tau & 0 \end{pmatrix} z\,, \quad (21)$$

where $z = [z_1 \;\; z_2 \;\; z_3]^T$ and parameter $\tau \in (-1, \;\infty)$.

Note that the first condition in the definition of the geometric Lorenz model is that the flow should have an equilibrium point O(0, 0, 0). If F denotes the vector field of the flow, then the derivative $DF(O)$ should have one positive eigenvalue $\lambda_1 > 0$ and two negative eigenvalues $\lambda_2 < \lambda_3 < 0$. Furthermore, the expanding eigenvalue should dominate the weakest contracting one, i.e. $\lambda_1 > -\lambda_3$. In fact, this is easily understood in view of the familiar Shilnikov's criterion [Shilnikov, 1993; Shilnikov *et al.*, 1993; Shilnikov, 1995; Shilnikov *et al.*, 2001].

The eigenvalues condition (20) is retained here in extending the concept of generalized Lorenz system:

Definition 2. The nonlinear system of ordinary differential equations in $\mathbf{R}^3$ of the following form is called a generalized Lorenz-like system:

$$\dot{x} = \begin{pmatrix} a_{11} & a_{12} & a_{13} \\ a_{21} & a_{22} & a_{23} \\ a_{31} & a_{32} & a_{33} \end{pmatrix} x + x_1 \begin{pmatrix} b_{11} & b_{12} & b_{13} \\ b_{21} & b_{22} & b_{23} \\ b_{31} & b_{32} & b_{33} \end{pmatrix} x + x_2 \begin{pmatrix} c_{11} & c_{12} & c_{13} \\ c_{21} & c_{22} & c_{23} \\ c_{31} & c_{32} & c_{33} \end{pmatrix} x + x_3 \begin{pmatrix} d_{11} & d_{12} & d_{13} \\ d_{21} & d_{22} & d_{23} \\ d_{31} & d_{32} & d_{33} \end{pmatrix} x, \quad (22)$$

where $x = [x_1 \;\; x_2 \;\; x_3]^T$, $A = (a_{ij})_{3\times 3}$, $B = (b_{ij})_{3\times 3}$, $C = (c_{ij})_{3\times 3}$ are all real matrixes, $b_{i2} = c_{i1}$, $b_{i3} = d_{i1}$, $c_{i3} = d_{i2}$ $(i = 1, 2, 3)$, and A has eigenvalues λ_1, λ_2, $\lambda_3 \in \mathbf{R}$ such that

$$-\lambda_2 > \lambda_1 > -\lambda_3 > 0\,. \quad (23)$$

Furthermore, the generalized Lorenz-like system is said to be nontrivial if it has at least one solution that goes neither to a limit cycle nor to zero or infinity.

The following theorem can be easily verified:

Theorem 6. *There exists a nonsingular linear change of coordinates, $z = Tx$, which takes (22) into the following generalized Lorenz-like canonical form*:

$$\dot{z} = \begin{pmatrix} \lambda_1 & 0 & 0 \\ 0 & \lambda_2 & 0 \\ 0 & 0 & \lambda_3 \end{pmatrix} z + ez\bar{B}z + fz\bar{C}z + gz\bar{D}z\,, \tag{24}$$

where $z = (z_1 \;\; z_2 \;\; z_3)^T$, *and*

$$\begin{gathered} \bar{B} = TBT^{-1}, \quad \bar{C} = TCT^{-1}, \quad \bar{D} = TDT^{-1}\,, \\ e = (1 \;\; 0 \;\; 0)T^{-1}, \quad f = (0 \;\; 1 \;\; 0)T^{-1}\,, \\ g = (0 \;\; 0 \;\; 1)T^{-1}\,. \end{gathered} \tag{25}$$

Proof. Direct computations show

$$\begin{aligned} \dot{z} = T\dot{x} &= T(Ax + x_1Bx + x_2Cx + x_3Dx) \\ &= TAT^{-1}z + T(1 \;\; 0 \;\; 0)T^{-1}zBT^{-1}z \\ &\quad + T(0 \;\; 1 \;\; 0)T^{-1}zCT^{-1}z \\ &\quad + T(0 \;\; 0 \;\; 1)T^{-1}zDT^{-1}z\,. \end{aligned}$$

Obviously, $(1 \;\; 0 \;\; 0)T^{-1}z$, $(0 \;\; 1 \;\; 0)T^{-1}z$, and $(0 \;\; 0 \;\; 1)T^{-1}z$ are scalar functions. Therefore, they are commutative with T. The proof is thus completed. ■

Remarks

(1) One can further simplify the *generalized Lorenz-like canonical* form (24) for some special cases, such as system (18), to get the simpler canonical form (21). In fact, since $\bar{A} = \mathrm{diag}\{\lambda_1, \lambda_2, \lambda_3\}$ is a diagonal matrix, $\bar{A}$ remains unchanged under the rest transformations. One can also simplify the matrixes $\bar{B}$, $\bar{C}$, $\bar{D}$ using some suitable transformations.

(2) The *generalized Lorenz-like system* (22) is not always chaotic under condition (23) for all system parameters. Actually, (23) is only a necessary condition for some chaotic systems.

(3) The *generalized Lorenz-like canonical form* provides a useful tool for studying chaos control and synchronization, chaotification, etc. Furthermore, system (24) gives a kind of unique and unified classification for a large class of chaotic systems.

9. Classification and Normal Form of Three-Dimensional Quadratic Autonomous Systems

In this section, some known three-dimensional quadratic autonomous chaotic systems are reviewed, followed by a classification and their normal forms [Chow *et al.*, 1994].

Recall that the celebrated Lorenz system is

$$\begin{cases} \dot{x} = a(y - x) \\ \dot{y} = cx - xz - y \\ \dot{z} = xy - bz\,. \end{cases} \tag{26}$$

When $a = 10$, $b = 8/3$, $c = 28$, system (26) has a 2-scroll chaotic attractor [Lorenz, 1963; Lofaro, 1997; Leonov, 2001; Magnitskii & Sidorov, 2001].

The Rössler system is

$$\begin{cases} \dot{x} = -y - z \\ \dot{y} = x + ay \\ \dot{z} = b + xz - cz\,, \end{cases} \tag{27}$$

which can display a single-folded band chaotic attractor when $a = b = 0.2$, $c = 5.7$.

The Rucklidge's system [Rucklidge, 1992] is a model of a double convection process, described by

$$\begin{cases} \dot{x} = ax - ly - yz \\ \dot{y} = x \\ \dot{z} = -z + y^2\,, \end{cases} \tag{28}$$

which has a 2-scroll chaotic attractor when $a = -2$, $l = -6.7$.

The Chen system, a *dual* system of the Lorenz system as discussed above, is described by:

$$\begin{cases} \dot{x} = a(y - x) \\ \dot{y} = (c - a)x - xz + cy \\ \dot{z} = xy - bz\,. \end{cases} \tag{29}$$

When $a = 35$, $b = 3$, $c = 28$, this system generates a complex 2-scroll chaotic attractor [Chen & Ueta, 1999; Ueta & Chen, 2000; Lü *et al.*, 2002g, 2002h; Chen & Lü, 2003].

The transition system coined by Lü and Chen [2002] bridges the gap between the Lorenz system and the Chen system, and its dynamical equations are

$$\begin{cases} \dot{x} = a(y - x) \\ \dot{y} = -xz + cy \\ \dot{z} = xy - bz\,. \end{cases} \tag{30}$$

This system displays a 2-scroll chaotic attractor when $a = 36$, $b = 3$, $c = 20$ [Lü & Chen, 2002; Lü *et al.*, 2002a, 2002b; Yu & Zhang, 2002, 2003; Zhou, 2002; Lü & Lu, 2003].

Moreover, Liu and Chen [2003] introduced the following simple system:

$$\begin{cases} \dot{x} = ax + d_1 yz \\ \dot{y} = by + d_2 xz \\ \dot{z} = cz + d_3 xy\,, \end{cases} \tag{31}$$

where $ab + ac + bc \neq 0$. It can create a complex 2- and 4-scroll attractors for the parameters: $d_1 = -1$, $d_2 = 1$, $d_3 = 1$, $a = 5$, $b = -10$, $c = -3.4$, and $d_1 = 1$, $d_2 = -1$, $d_3 = -1$, $a = 0.5$, $b = -10$, $c = -4$, respectively.

Also, the new chaotic system introduced above in this article is

$$\begin{cases} \dot{x} = -\dfrac{ab}{a+b}x - yz + c \\ \dot{y} = ay + xz \\ \dot{z} = bz + xy\,, \end{cases} \tag{32}$$

which can display two 1-scroll chaotic attractors simultaneously for $a = -10$, $b = -4$, $c = 18.1$, and two 2-scroll chaotic attractors simultaneously for $a = -10$, $b = -4$, $c = 0$.

Sprott found 19 algebraically simple chaotic systems by exhaustive computer searching as follows [Sprott, 1994, 1997; Sprott & Linz, 2000; Linz & Sprott, 1999]: The first one is

$$\begin{cases} \dot{x} = y \\ \dot{y} = -x + yz \\ \dot{z} = 1 - y^2\,. \end{cases} \tag{33}$$

But Hoover [1995] pointed out that system (33) is a special case of the Nosé–Hoover thermostated dynamic system that had earlier been shown to exhibit time-reversible Hamiltonian chaos [Posch *et al.*, 1986]. And the other 18 are:

$$\begin{cases} \dot{x} = yz \\ \dot{y} = x - y \\ \dot{z} = 1 - xy\,, \end{cases} \tag{34}$$

$$\begin{cases} \dot{x} = yz \\ \dot{y} = x - y \\ \dot{z} = 1 - x^2\,, \end{cases} \tag{35}$$

$$\begin{cases} \dot{x} = -y \\ \dot{y} = x + z \\ \dot{z} = xz + 3y^2\,, \end{cases} \tag{36}$$

$$\begin{cases} \dot{x} = yz \\ \dot{y} = x^2 - y \\ \dot{z} = 1 - 4x\,, \end{cases} \tag{37}$$

$$\begin{cases} \dot{x} = y + z \\ \dot{y} = -x + 0.5y \\ \dot{z} = x^2 - z\,, \end{cases} \tag{38}$$

$$\begin{cases} \dot{x} = 0.4x + z \\ \dot{y} = xz - y \\ \dot{z} = -x + y\,, \end{cases} \tag{39}$$

$$\begin{cases} \dot{x} = -y + z^2 \\ \dot{y} = x + 0.5y \\ \dot{z} = x - z\,, \end{cases} \tag{40}$$

$$\begin{cases} \dot{x} = -0.2y \\ \dot{y} = x + z \\ \dot{z} = x + y^2 - z\,, \end{cases} \tag{41}$$

$$\begin{cases} \dot{x} = 2z \\ \dot{y} = -2y + z \\ \dot{z} = -x + y + y^2\,, \end{cases} \tag{42}$$

$$\begin{cases} \dot{x} = xy - z \\ \dot{y} = x - y \\ \dot{z} = x + 0.3z\,, \end{cases} \tag{43}$$

$$\begin{cases} \dot{x} = y + 3.9z \\ \dot{y} = 0.9x^2 - y \\ \dot{z} = 1 - x\,, \end{cases} \tag{44}$$

$$\begin{cases} \dot{x} = -z \\ \dot{y} = -x^2 - y \\ \dot{z} = 1.7 + 1.7x + y\,, \end{cases} \tag{45}$$

$$\begin{cases} \dot{x} = -2y \\ \dot{y} = x + z^2 \\ \dot{z} = 1 + y - 2z\,, \end{cases} \tag{46}$$

$$\begin{cases} \dot{x} = y \\ \dot{y} = x - z \\ \dot{z} = x + xz + 2.7y\,, \end{cases} \tag{47}$$

$$\begin{cases} \dot{x} = 2.7y + z \\ \dot{y} = -x + y^2 \\ \dot{z} = x + y\,, \end{cases} \tag{48}$$

$$\begin{cases} \dot{x} = -z \\ \dot{y} = x - y \\ \dot{z} = 3.1x + y^2 + 0.5z\,, \end{cases} \tag{49}$$

$$\begin{cases} \dot{x} = 0.9 - y \\ \dot{y} = 0.4 + z \\ \dot{z} = xy - z\,, \end{cases} \tag{50}$$

$$\begin{cases} \dot{x} = -x - 4y \\ \dot{y} = x + z^2 \\ \dot{z} = 1 + x\,, \end{cases} \tag{51}$$

It is noticed that the Rössler attractor and Sprott's attractors of Eqs. (33)–(51) are all topologically simpler than the 2-scroll Lorenz attractor. Furthermore, Sprott's attractors behave similarly in that they all tend to resemble the single-fold band structure of the Rössler attractor.

Genesio and Tesi [1992] discussed the following system:

$$\begin{cases} \dot{x} = y \\ \dot{y} = z \\ \dot{z} = -cx - by - az + x^2\,, \end{cases} \tag{52}$$

where the parameters a, b, c satisfy $ab < c$. When $a = 0.44$, $b = 1.1$, $c = 1$, system (52) displays a typical chaotic attractor.

The dynamical equations of the Shimizu–Morioka model are

$$\begin{cases} \dot{x} = y \\ \dot{y} = x - ay - xz \\ \dot{z} = -bz + x^2\,, \end{cases} \tag{53}$$

where the parameters $a > 0$, $b > 0$. System (53) shows a chaotic attractor for $a = 0.85$, $b = 0.5$.

A low-order atmospheric circulation model is described by

$$\begin{cases} \dot{x} = -ax - y^2 - z^2 + aF \\ \dot{y} = -y + xy - bxz + G \\ \dot{z} = -z + bxy + xz\,, \end{cases} \tag{54}$$

where x represents the strength of the globally averaged westerly current, and y, z are the strength of the cosine and sine phases of a chain of superposed waves. The unit of the variable t is equal to the damping time of the waves, estimated to be five days. The terms in F and G represent thermal forcing terms, and the parameter b stands for the strength of the advection of the waves by the westerly current. Here, F, G are treated as control parameters, with $a = 1/4$, $b = 4$ [Shilnikov *et al.*, 1995]. System (54) is also called a new Lorenz model.

Given all the above models, the three-dimensional quadratic autonomous chaotic systems are now classified as follows.

Case A. System properties

- Dissipative chaotic systems, such as systems (26)–(32) and (34)–(54).
- Conservative chaotic systems, the only known system is (33).

Case B. Topological structure of attractor

- One 1-scroll or single-fold band structure, such as the Rössler attractor and Sprott's attractors.
- One 2-scroll structure, such as the Lorenz attractor, Chen attractor, transition system attractor, and Rucklidge's attractor.
- One 4-scroll structure, such as system (31).
- Two 1-scroll structures, such as system (32).
- Two 2-scroll structures, such as system (32).

Remark

- Obviously, system (32) has two typical new topological structures — two 1-scroll structures and two 2-scroll structures. Up to now, it is not known if three-dimensional quadratic autonomous chaotic systems have more complicated topological structures in this classification.

In the following, equilibria and eigenvalues for several typical chaotic systems are summarized in Table 5.

Remarks

(1) Obviously, the Lorenz system, Rucklidge system, Chen system, transition system, system (31), and Shimizu–Morioka model belong to the generalized Lorenz-like system of Definition 2. Furthermore, the Lorenz, Chen and transition systems are also generalized Lorenz system of Definition 1. Therefore, the concept of generalized Lorenz-like system is more general than that of generalized Lorenz system.

(2) However, the Rössler system, system (1), and the Genesio–Tesi system do not belong to the generalized Lorenz-like system. Especially, when $a = -10$, $b = -4$, $c = 0$, the expanding eigenvalue does not dominate the weakest contracting one in system (1), that is,

$-(-10) > -(-4) > 2.8571$. This is quite a special phenomenon for three-dimensional quadratic autonomous chaotic systems.

Consider the following general three-dimensional quadratic autonomous system:

$$\dot{X} = AX + xBX + yCX + zDX + E\,, \qquad (55)$$

where $X = (x\ y\ z)^T$, $A = (a_{ij})_{3\times3}$, $B = (b_{ij})_{3\times3}$, $C = (c_{ij})_{3\times3}$, $D = (d_{ij})_{3\times3}$, and $E = (e_1\ e_2\ e_3)^T$ are all real matrices, and matrices B, C, D satisfy $b_{i2} = c_{i1}$, $b_{i3} = d_{i1}$, $c_{i3} = d_{i2}$ $(i = 1, 2, 3)$.

In order to further investigate the dynamical behaviors of system (55), the matrix A can be transformed into the Jordan normal form. For example, consider the following transformation of the Lorenz system (26):

$$x = u + v,\quad a(y - x) = \lambda_1 u + \lambda_2 v,\quad z = z\,,$$

where λ_1, λ_2 are roots of the equation

$$\lambda^2 + (a + 1)\lambda - a(c - 1) = 0\,. \qquad (56)$$

Then, system (26) takes the new form

$$\begin{cases} \dot{u} = \lambda_1 u + \dfrac{az(u + v)}{\lambda_2 - \lambda_1} \\ \dot{v} = \lambda_2 v - \dfrac{az(u + v)}{\lambda_2 - \lambda_1} \\ \dot{z} = -bz + (u + v)^2 + \dfrac{1}{a}(u + v)(\lambda_1 u + \lambda_2 v)\,. \end{cases} \qquad (57)$$

The notion of Lorenz equations in the variables (u, v, z) is more convenient than the corresponding notion in the variables (x, y, z), since for any c, the stable manifold W^s of the origin is tangent to the u-axis and the unstable manifold W^u is tangent to the v-axis. This demonstrates clearly many new important characteristics of the attractor, which are invariant with respect to the parameter c [Jones *et al.*, 1985; Magnitskii & Sidorov, 2001]. Furthermore, there are other canonical forms that can be used for studying the dynamical behaviors of the Lorenz system, such as the canonical form suggested by Čelikovský and Chen [2002, 2003].

Lemma 2. *For any real matrix $A = (a_{ij})_{3\times3}$, let λ_1, λ_2, λ_3 be its eigenvalues. Then,*

Table 5. Equilibria and eigenvalues for several typical chaotic systems.

System	Parameters	Equilibria	Eigenvalues
Lorenz system	$a = 10,\ b = \frac{8}{3},\ c = 28$	$(0,\ 0,\ 0)$	$-22.8277,\ -2.6667,\ 11,8277$
		$(\pm6\sqrt{2},\ \pm6\sqrt{2},\ 27)$	$-13.8546,\ 0.0940 \pm 0.1945\,i$
Rössler system	$a = b = 0.2,\ c = 5.7$	$(0.0070,\ -0.0351,\ 0.0351)$	$-5.6870,\ 0.0970 \pm 0.9952\,i$
		$(5.6930,\ -28.4649,\ 28.4649)$	$-4.6 \times 10^{-6},\ 0.1930 \pm 5.4280\,i$
Rucklidge system	$a = -2,\ l = -6.7$	$(0,\ 0,\ 0)$	$-3.7749,\ -1,\ 1.7749$
		$(0,\ \pm2.5884,\ 6.7)$	$-3.5154,\ 0.2577 \pm 1.9353\,i$
Chen system	$a = 35,\ b = 3,\ c = 28$	$(0,\ 0,\ 0)$	$-30.8359,\ -3,\ 23.8359$
		$(\pm3\sqrt{7},\ \pm3\sqrt{7},\ 21)$	$-18.4288,\ 4.2140 \pm 14.8846\,i$
Transition system	$a = 36,\ b = 3,\ c = 20$	$(0,\ 0,\ 0)$	$-36,\ -3,\ 20$
		$(\pm2\sqrt{15},\ \pm2\sqrt{15},\ 20)$	$-22.6516,\ 1.8258 \pm 13.6887\,i$
System (31)	$a = 5,\ b = -10,\ c = -3.4$	$(0,\ 0,\ 0)$	$-10,\ -3.4,\ 5$
	$d_1 = -1,\ d_2 = d_3 = 1$	$(\sqrt{34},\ \pm\sqrt{17},\ \pm5\sqrt{2})$	$-12.6496,\ 2.1248 \pm 7.0172\,i$
		$(-\sqrt{34},\ \pm\sqrt{17},\ \mp5\sqrt{2})$	
System (1)	$a = -10,\ b = -4,\ c = 18.1$	$(-6.335,\ 0,\ 0)$	$-14.0094,\ 0.0094,\ 2.8571$
		$(2\sqrt{10},\ \pm4.7829,\ \pm7.5624)$	$-13.3021,\ 1.0796 \pm 8.2233\,i$
	$a = -10,\ b = -4,\ c = 0$	$(0,\ 0,\ 0)$	$-10,\ -4,\ 2.8571$
		$(2\sqrt{10},\ \pm\frac{4}{7}\sqrt{35},\ \pm\frac{10}{7}\sqrt{14})$	$-13.6106,\ 1.2339 \pm 5.6626\,i$
		$(-2\sqrt{10},\ \pm\frac{4}{7}\sqrt{35},\ \mp\frac{10}{7}\sqrt{14})$	
Genesio–Tesi system	$a = 0.44,\ b = 1.1,\ c = 1$	$(0,\ 0,\ 0)$	$-0.7503,\ 0.1551 \pm 1.1440\,i$
		$(1,\ 0,\ 0)$	$0.5872,\ -0.5136 \pm 1.1997\,i$
Shimizu–Morioka model	$a = 0.85,\ b = 0.5$	$(0,\ 0,\ 0)$	$-1.5116,\ -0.5,\ 0.6616$
		$(\pm\frac{1}{2}\sqrt{2},\ 0,\ 1)$	$-1.5079,\ 0.0790 \pm 0.8105\,i$

(1) *If* $\lambda_1, \lambda_2, \lambda_3 \in \mathbf{R}$ *and* $\lambda_1 \neq \lambda_2$, $\lambda_1 \neq \lambda_3$, $\lambda_2 \neq \lambda_3$, *then there exists a nonsingular real matrix* T *such that*

$$\bar{A} = TAT^{-1} = \begin{pmatrix} \lambda_1 & 0 & 0 \\ 0 & \lambda_2 & 0 \\ 0 & 0 & \lambda_3 \end{pmatrix}; \quad (58)$$

(2) *If* $\lambda_1, \lambda_2, \lambda_3 \in \boldsymbol{R}$ *and* $\lambda_1 = \lambda_2 \neq \lambda_3$, *then there exists a nonsingular real matrix* T *such that*

$$\bar{A} = TAT^{-1} = \begin{pmatrix} \lambda_1 & 0 & 0 \\ 0 & \lambda_1 & 0 \\ 0 & 0 & \lambda_3 \end{pmatrix}$$

$$or \quad \begin{pmatrix} \lambda_1 & 1 & 0 \\ 0 & \lambda_1 & 0 \\ 0 & 0 & \lambda_3 \end{pmatrix}; \quad (59)$$

(3) *If* $\lambda_1 = \lambda_2 = \lambda_3 \in \mathbf{R}$, *then there exists a nonsingular real matrix* T *such that*

$$\bar{A} = TAT^{-1} = \begin{pmatrix} \lambda_1 & 0 & 0 \\ 0 & \lambda_1 & 0 \\ 0 & 0 & \lambda_1 \end{pmatrix}$$

$$or \quad \begin{pmatrix} \lambda_1 & 1 & 0 \\ 0 & \lambda_1 & 0 \\ 0 & 0 & \lambda_1 \end{pmatrix}$$

$$or \quad \begin{pmatrix} \lambda_1 & 1 & 0 \\ 0 & \lambda_1 & 1 \\ 0 & 0 & \lambda_1 \end{pmatrix}; \quad (60)$$

(4) *If* $\lambda_1 = \alpha + \beta i$, $\alpha, \beta, \lambda_3 \in \mathbf{R}$, *then there exists a nonsingular real matrix* T *such that*

$$\bar{A} = TAT^{-1} = \begin{pmatrix} \alpha & -\beta & 0 \\ \beta & \alpha & 0 \\ 0 & 0 & \lambda_3 \end{pmatrix}. \quad (61)$$

Proof. It follows from straightforward computations. ■

Therefore, the following theorem is immediate:

Theorem 7. *For any three-dimensional quadratic autonomous system in the form of* (55), *there exists a nonsingular linear transformation,* $U = TX$, *which takes* (55) *into the following canonical form*:

$$\dot{U} = \bar{A} + fU\bar{B}U + gU\bar{C}U + hU\bar{D}U + \bar{E}, \quad (62)$$

where $U = (u \;\; v \;\; w)^T$, *and*

$$\begin{gathered} \bar{B} = TBT^{-1}, \quad \bar{C} = TCT^{-1}, \\ \bar{D} = TDT^{-1}, \quad \bar{E} = TE, \\ f = (1 \;\; 0 \;\; 0)T^{-1}, \quad g = (0 \;\; 1 \;\; 0)T^{-1}, \\ h = (0 \;\; 0 \;\; 1)T^{-1}. \end{gathered} \quad (63)$$

Similar to Theorem 6, a proof follows from straightforward computations.

Remarks

(1) If system (55) is chaotic, then $\bar{A}$ is not in the form of (60). Otherwise, one has $\nabla V = (\partial\dot{x}/\partial x) + (\partial\dot{y}/\partial y) + (\partial\dot{z}/\partial z) = 3\lambda_1 < 0$, so the equilibrium point is stable but it is impossible.
(2) If system (55) is chaotic and $\bar{A}$ is in the form of (58), then $\lambda_1 + \lambda_2 + \lambda_3 < 0$, $\lambda_1 > 0$, $\lambda_3 < 0$ $(\lambda_1 \geq \lambda_2 \geq \lambda_3)$.
(3) One can further simplify the canonical form (62) for some special cases, such as system (18), for which it takes the simpler canonical form (21).
(4) The canonical form (62) is very convenient for discussing the dynamical behavior of chaotic systems.

10. Conclusions and Discussion

It came as a big surprise to most scientists when Lorenz discovered chaos in a simple system of three-dimensional quadratic autonomous ordinary differential equations in 1963. For nearly 40 years, many simple chaotic flows have been found and further studied within the framework of three-dimensional quadratic autonomous systems. These simple chaotic systems have stimulated a great deal of interest in the studies of chaotic dynamics from a unified point of view, as well as related chaos control and synchronization problems.

This article has presented and further studied a new chaotic system of three-dimensional quadratic autonomous equations, which can generate two 1-scroll chaotic attractors simultaneously with three equilibria, and two 2-scroll chaotic attractors simultaneously with five equilibria. Dynamical behaviors of this new chaotic system, including some basic dynamical properties, bifurcations, periodic windows, routes to chaos, compound structures of the new attractors and their connections, etc. have been investigated both theoretically and numerically. Moreover, the concept of generalized Lorenz system has been further extended, so is the notion of generalized Lorenz-like systems. Some discussion of a simple classification and normal form has been carried out for these three-dimensional quadratic autonomous chaotic systems.

It has become clearer today that even the relatively simple three-dimensional quadratic autonomous chaotic systems are still demanding

more efforts of deeper investigation. Besides their abundant and complex dynamical behaviors, the intrinsic relations among them in a better and more complete classification remain an interesting topic for further research. It has also become clearer today that following some basic ideas and techniques of chaotification, more and more new chaotic systems, especially unknown members of the elementary class of three-dimensional quadratic autonomous chaotic systems, can be found and will be found intentionally. This will greatly enhance our understanding of chaotic systems in general, and benefit chaotic dynamics analysis as well as chaos control and synchronization with sensible engineering applications in particular.

Acknowledgments

The authors would like to thank Dr. Radoslav Radev for his interest in this paper. This work was partly supported by Hong Kong Research Grants Council under Grants CityU, 1018/01E, 1004/02E, and 1115/03E the K. C. Wong Education Foundation, Hong Kong, the Chinese Postdoctoral Scientific Foundation, and the National Natural Science Foundation of China No. 60304017.

References

Arneodo, A., Coullet, P. H., Spiegel, E. A. & Tresser, C. [1985] "Asymptotic chaos," *Physica* **D14**, 327–347.

Čelikovský, S. & Chen, G. [2002] "On a generalized Lorenz canonical form of chaotic systems," *Int. J. Bifurcation and Chaos* **12**, 1789–1812.

Čelikovský, S. & Chen, G. [2003] "Hyperbolic-type generalized Lorenz chaotic system and its canonical form," *Proc. 15th IFAC Triennial World Congress on Automatic Control* (*IFAC'02*), Barcelona, Spain, 22–27 July 2002, published in CDROM.

Chen, G. [1993] "Controlling Chua's global unfolding circuit family," *IEEE Trans. Circuits Syst.-I* **40**, 829–832.

Chen, G. & Dong, X. [1998] *From Chaos to Order: Methodologies, Perspectives and Applications* (World Scientific, Singapore).

Chen, G. & Lai, D. [1998] "Anticontrol of chaos via feedback," *Int. J. Bifurcation and Chaos* **8**, 1585–1590.

Chen, G. [1999] *Controlling Chaos and Bifurcations in Engineering Systems* (CRC Press, Boca Raton, FL).

Chen, G. & Ueta, T. [1999] "Yet another chaotic attractor," *Int. J. Bifurcation and Chaos* **9**, 1465–1466.

Chen, G. & Lü, J. [2003] *Dynamical Analysis, Control and Synchronization of the Generalized Lorenz Systems Family* (in Chinese) (Science Press, Beijing).

Chow, S., Li, C. & Wang, D. [1994] *Normal Forms and Bifurcation of Planar Vector Fields* (Cambridge University Press, Cambridge).

Deng, B. [1995] "Constructing Lorenz type attractors through singular perturbations," *Int. J. Bifurcation and Chaos* **5**, 1633–1642.

Elwakil, A. S. & Kennedy, M. P. [2001] "Construction of classes of circuit-independent chaotic oscillators using passive-only nonlinear devices," *IEEE Trans. Circuits Syst.-I* **48**, 289–307.

Elwakil, A. S., Özoguz, S. & Kennedy, M. P. [2002] "Creation of a complex butterfly attractor using a novel Lorenz-type system," *IEEE Trans. Circuits Syst.-I* **49**, 527–530.

Festa, R., Mazzino, A. & Vincenzi, D. [2002] "Lorenz-like systems and classical dynamical equations with memory forcing: An alternate point of view for singling out the origin of chaos," *Phys. Rev.* **E65**, 046205.

Funakoshi, M. [2001] "Lagrangian chaos and mixing of fluids," *Japan J. Indus. Appl. Math.* **18**, 613–626.

Genesio, R. & Tesi, A. [1992] "Harmonic balance methods for the analysis of chaotic dynamics in nonlinear systems," *Automatica* **28**, 531–548.

Hao, B. L. [1984] *Chaos* (World Scientific, Singapore).

Hoover, W. G. [1995] "Remark on 'Some simple chaotic flows'," *Phys. Rev.* **E51**, 759–760.

Jack, H. & Zhang, F. [1999] "Nonchaotic behaviour in three-dimensional quadratic systems II. The conservative case," *Nonlinearity* **12**, 617–633.

Jones, C. A., Weiss, N. O. & Cattaneo, F. [1985] "Nonlinear dynamos: A complex generalization of the Lorenz equations," *Physica* **D14**, 161–176.

Leonov, G. A. [2001] "Bounds for attractors and the existence of homoclinic orbits in the Lorenz system," *J. Appl. Math. Mechs.* **65**, 19–32.

Linz, S. J. & Sprott, J. C. [1999] "Elementary chaotic flow," *Phys. Lett.* **A259**, 240–245.

Liu, W. B. & Chen, G. [2003] "A new chaotic system and its generation," *Int. J. Bifurcation and Chaos* **12**, 261–267.

Lofaro, T. [1997] "A model of the dynamics of the Newton–Leipnik attractor," *Int. J. Bifurcation and Chaos* **7**, 2723–2733.

Lorenz, E. N. [1963] "Deterministic nonperiodic flow," *J. Atmos. Sci.* **20**, 130–141.

Lorenz, E. N. [1993] *The Essence of Chaos* (University of Washington Press, Seattle), p. 148.

Lü, J. & Chen, G. [2002] "A new chaotic attractor coined," *Int. J. Bifurcation and Chaos* **12**, 659–661.

Lü, J., Chen, G., Cheng, D. & Čelikovský, S. [2002a] "Bridge the gap between the Lorenz system and the Chen system," *Int. J. Bifurcation and Chaos* **12**, 2917–2926.

Lü, J., Chen, G. & Zhang, S. [2002b] "Dynamical analysis of a new chaotic attractor," *Int. J. Bifurcation and Chaos* **12**, 1001–1015.

Lü, J., Chen, G. & Zhang, S. [2002c] "The compound structure of a new chaotic attractor," *Chaos Solit. Fract.* **14**, 669–672.

Lü, J., Chen, G. & Zhang, S. [2002d] "Controlling in between the Lorenz and the Chen systems," *Int. J. Bifurcation and Chaos* **12**, 1417–1422.

Lü, J., Lu, J. & Chen, S. [2002e] *Chaotic Time Series Analysis and Its Applications* (in Chinese) (Wuhan University Press, Wuhan, China).

Lü, J., Zhou, T., Chen, G. & Yang, X. [2002f] "Generating chaos with a switching piecewise-linear controller," *Chaos* **12**, 344–349.

Lü, J., Zhou, T., Chen, G. & Zhang, S. [2002g] "The compound structure of Chen's attractor," *Int. J. Bifurcation and Chaos* **12**, 855–858.

Lü, J., Zhou, T., Chen, G. & Zhang, S. [2002h] "Local bifurcation of the Chen system," *Int. J. Bifurcation and Chaos* **12**, 2257–2270.

Lü, J. & Lu, J. [2003] "Controlling uncertain Lü system using linear feedback," *Chaos Solit. Fract.* **17**, 127–133.

Lü, J., Yu, X. & Chen, G. [2003] "Generating chaotic attractors with multiple merged basins of attraction: A switching piecewise-linear control approach," *IEEE Trans. Circuits Syst.-I* **50**, 198–207.

Magnitskii, N. A. & Sidorov, S. V. [2001] "A new view of the Lorenz attractor," *Diff. Eqs.* **37**, 1494–1506.

Ott, E., Grebogi, C. & Yorke, J. A. [1990] "Controlling chaos," *Phys. Rev. Lett.* **64**, 1196–1199.

Posch, H. A., Hoover, W. G. & Vesely, F. J. [1986] "Canonical dynamics of the Nosé oscillator: Stability, order, and chaos," *Phys. Rev.* **A33**, 4253–4265.

Rössler, O. E. [1976] "An equation for continuous chaos," *Phys. Lett.* **A57**, 397–398.

Rössler, O. E. [1979] "Continuous chaos — four prototype equations," *Ann. (N. Y.) Acad. Sci.* **316**, 376–392.

Rucklidge, A. M. [1992] "Chaos in models of double convection," *J. Fluid Mech.* **237**, 209–229.

Schmalzl, J. Houseman, G. A. & Hansen, U. [1995] "Mixing properties of three-dimensional (3-D) stationary convection," *Phys. Fluids* **7**, 1027–1033.

Shilnikov, A. L. [1993] "On bifurcations of the Lorenz attractor in the Shimizu–Morioka model," *Physica* **D62**, 338–346.

Shilnikov, A. L., Shilnikov, L. P. & Turaev, D. V. [1993] "Normal forms and Lorenz attractors," *Int. J. Bifurcation and Chaos* **5**, 1123–1139.

Shilnikov, A., Nicolis, G. & Nicolis, C. [1995] "Bifurcation and predictability analysis of a low-order atmospheric circulation model," *Int. J. Bifurcation and Chaos* **5**, 1701–1711.

Shilnikov, L. P., Shilnikov, A. L., Turaev, D. V. & Chua, L. O. [2001] *Methods of Qualitative Theory in Nonlinear Dynamics Part II* (World Scientific, Singapore).

Smale, S. [2000] "Mathematical problems for the next century," *Mathematics: Frontiers and Perspectives*, January Issue, 271–294.

Sprott, J. C. [1994] "Some simple chaotic flows," *Phys. Rev.* **E50**, R647–R650.

Sprott, J. C. [1997] "Simplest dissipative chaotic flow," *Phys. Lett.* **A228**, 271–274.

Sprott, J. C. & Linz, S. J. [2000] "Algebraically simple chaotic flows," *Int. J. Chaos Th. Appl.* **5**, 3–22.

Stewart, I. [2002] "The Lorenz attractor exists," *Nature* **406**, 948–949.

Suykens, J. A. K. & Vandewalle, J. [1993] "Generation of n-double scrolls ($n = 1, 2, 3, 4, \ldots$)," *IEEE Trans. Circuits Syst.-I* **40**, 861–867.

Tang, K. S., Man, K. F., Zhong, G. Q. & Chen, G. [2001] "Generating chaos via $x|x|$," *IEEE Trans. Circuits Syst.-I* **48**, 636–641.

Tang, K. S., Man, K. F., Zhong, G. Q. & Chen, G. [2002] "Some new circuit design for chaos generation," in *Chaos in Circuits and Systems*, ed. Chen, G. & Ueta, T. (World Scientific, Singapore), pp. 171–190.

Tucker, W. [1999] "The Lorenz attractor exists," *C. R. Acad. Sci. Paris* **328**, 1197–1202.

Ueta, T. & Chen, G. [2000] "Bifurcation analysis of Chen's attractor," *Int. J. Bifurcation and Chaos* **10**, 1917–1931.

Vaněček, A. & Čelikovský, S. [1996] *Control Systems: From Linear Analysis to Synthesis of Chaos* (Prentice-Hall, London).

Wang, X. & Chen, G. [1999] "On feedback anticontrol of discrete chaos," *Int. J. Bifurcation and Chaos* **9**, 1435–1441.

Wang, X. & Chen, G. [2000] "Chaotification via arbitrarily small feedback controls: Theory, method, and applications," *Int. J. Bifurcation and Chaos* **10**, 549–570.

Wang, X., Chen, G. & Yu, X. [2000] "Anticontrol of chaos in continuous-time systems via time-delayed feedback," *Chaos* **10**, 771–779.

Wiggins, S. [1990] *Introduction to Applied Nonlinear Dynamical Systems and Chaos* (Springer, NY).

Yang, X. S. & Chen, G. [2002] "On non-chaotic behavior of a class of jerky systems," *Far East J. Dyn. Syst.* **4**, 27–38.

Yu, Y. & Zhang, S. [2002] "Adaptive backstepping control of the uncertain Lü system," *Chinese Phys.* **11**, 1249–1253.

Yu, Y. & Zhang, S. [2003] "Controlling uncertain Lü system using backstepping design," *Chaos Solit. Fract.* **15**, 897–902.

Zhang, F. & Jack, H. [1997] "Non-chaotic behavior in three-dimensional quadratic systems," *Nonlinearity* **10**, 1289–1303.

Zhou, Z. [2002] "A new chaotic anti-control model – Lü system," *J. Xianning Teachers College* **22**, 19–21.